# Feedback between ecological interaction and spatial pattern in a transitional Michigan forest

by

David Nicoletti Allen

A dissertation submitted in partial fulfillment
of the requirements for the degree of
Doctor of Philosophy
(Ecology and Evolutionary Biology)
in The University of Michigan
2012

Doctoral Committee:

Professor John H. Vandermeer, Chair
Associate Professor Christopher William Dick
Associate Professor Aaron Alan King
Assistant Professor Inés Ibáñez

# ACKNOWLEDGEMENTS

Over the past six years I received an incredible amount of support from the Department of Ecology and Evolutionary Biology. The graduate students, post-docs, faculty, and staff in the department form an amazing intellectual and social community.

The support staff at EEB has been very helpful. They made many number things run smoothly, often in spite of me getting forms in late or making things needlessly complicated. Thanks especially to Jane Sullivan, Sonja Bottes, Amber Stadler, Ed Grant, and Sheila Dunn.

My committee provided guidance through the process and helpful comments for my dissertation. Thanks to Aaron King, Chris Dick and Inés Ibáñez.

A number of undergraduates helped me collect the Big Woods data during the 2008 and 2010 summers. They did so with great care and good spirit, I would like to thank them: Kate Zemenick, Richard Byler, Jordan Trejo, Margolit Sands, David Merian, and Benjamin Crotte.

In 2008, 2009, 2010, and 2011 I GSIed Field Ecology. The students in those courses had invaluable advice for my research, helped collect some data, and were generally great people who made six weekends a year spent at the ESGR very enjoyable. I would specifically like to thank Daniel Poon, Alexa Unruh, Aaron Iverson, Elizabeth Hood, Kelvin Hyunmin Han, Jes Skillman, Kariana Laneri and John Berini from the 2009 class who collected the branch data for Chapter V. Ivette Perfecto who, with John Vandermeer, was one of the Field Ecology professors was a great help to my

dissertation.

The Vandermeer and Perfecto labs have been an amazing group to work with. Their level of intellectual curiosity, political engagement, and dedication to their work has been an inspiration. They have also been very good friends. Over the years I have overlapped with a huge number: Stacy Philpott, Jahi Chappell, Zach Miller, Javier Ruiz, Krista McGuire, Heidi Liere, Shalene Jha, Katie Goodall, Doug Jackson, Heather Briggs, Julie Cotton, Casey Taylor, Kate Ennis, Aley Joseph, Hsun-Yi Hsieh, Andy MacDonald, Linda Marín, David Gonthier, Colin Donihue, Stacy Mates, Jes Skillman, Jane Remfert, Theresa Wei Ying Ong, Senay Yitbarek, Aaron Iverson, Iracenir A. Dos Santos, Sahar Haghighat, and William Webb.

I have had an incredible network of friends and family who have listened to me talk about my research for the past six, or eight if you count when I started in the math department, years. Sourya Shrestha has also been in Ann Arbor since 2003 (when we started in the math department together) and has been a good friend for that time. Anne Lippert has been a huge emotional and intellectual support through the years. My family–Mom, Dad, Dan, and Julie—and friends from Springfield—Emily, John, Trav, and Jennie—have also been helped me on the path to my dissertation.

I would like to recall the memories of the late Beverly Ratchke and George Estabrook, professors in EEB. They both played an important role in my time here. Beverly taught the first course I took in EEB, Plant-Animal Interactions, which I took when I was in the math department and helped propel me to EEB. George taught Practical Botany which I GSIed four times. I enjoyed the course very much and George was a big part of that. I miss them both dearly.

Finally, and most of all, I would like to thank my advisor John Vandermeer. He has been an amazing force in my life—as a scientific and intellectual advisor, as inspiration for how passion and principles structuring one's life, and as a good friend—for these past six years.

# TABLE OF CONTENTS

# LIST OF FIGURES

**Figure**

# LIST OF TABLES

**Table**

# ABSTRACT

Feedback between ecological interaction and spatial pattern in a transitional Michigan forest

by

David Nicoletti Allen

Chair: John H. Vandermeer

Ecology has traditionally thought of spatial patterns in one of two ways: (1) as a consequence of some underlying environmental heterogeneity and (2) as something to ignore in models to make them more tractable. But both of these views have changed, and in the last 20 years ecologists have increasingly considered the joint feedback that spatial pattern and ecological interactions can have on each other. Going in one direction the spatial pattern of organisms can greatly affect how their ecological interactions play out, and in the other direction local-scale ecological interactions can give rise to emergent, self-organized spatial patterns of organisms. This dissertation examines both directions of this feedback in the context of a mid-successional Michigan forest. The three dominant species in the understory of the forest exhibit strong nonrandom spatial patterning. Here we suggest that this spatial pattern emerges from biotic interactions—the combined effect of local dispersal and Janzen-Connell, density-dependent seed and seedling mortality of two of these three species—acting on an initial distribution of trees determined by the fire history of the area. That is ecological interactions give rise to spatial pattern, but this can only be understood

in light of the history of the forest. We also suggest that this spatial pattern will affect how the succession of the forest; if the species were completely well-mixed the succession of the forest would take place differently. So we show that the spatial arrangement of organisms affects ecological processes.

# CHAPTER I

# Introduction

Recently there has been a growing appreciation of the joint feedback between ecological interactions among organisms and the spatial arrangement of those organisms. This feedback is known to go in either or both directions: (1) ecological interactions can give rise to spatial patterns of organisms, and (2) the spatial pattern of organisms can have a large effect on how ecological interactions play out.

The understanding of (1) in ecology is, largerly, rather recent—with some important exceptions such as Janzen (1970) and Connell (1971). Historically spatial patterns in ecological systems have been thought to be solely the result of environmental, or exogenous, factors (e.g., soil, moisture, topography, ...), but we now appreciate that ecological interactions can form self-organized, or endogenous, pattern. This insight first discovered by Turing (1952) has been appreciated in chemistry (Castets et al., 1990) and developmental biology (Murray, 1981) for some time, but has only come to ecology in the past two decades (Solé and Manrubia, 1995; Klausmeier, 1999; Pascual et al., 2002; Rietkerk et al., 2002).

The understanding of (2) is older. In a classic experiment, Huffaker (1958) demonstrated that the spatial arrangement of habitats allowed an otherwise unstable predator-prey system to persist. Still most ecological theory—with the important exceptions of island biogeography and metapopulation theory—assumed a homogenous

arrangement of organisms, largely a contrivance for mathematical tractability. But this assumption has been relaxed in some recent literature. With new mathematical techniques and increased computing power, ecological theory increasingly considers the effects of non-random spatial patterns. These effects can be dramatic, having fundamental impacts on how competitive (Molofsky and Bever, 2002), predator-prey (Pascual, 1999), and host-parasite (Rohani et al., 1994) interactions play out.

In this dissertation I examine the two directions of this feedback, first the generation of pattern through ecological processes, and second the consequences of this pattern on ecological processes, using a mid-succession northeastern North American forest as a case study. This forest is of particular interest because it has a strongly spatially structured understory and is undergoing a dramatic shift in species composition—the same seen in many northeastern North American forests (Abrams, 1992, 1998; Zhang et al., 2000; McDonald et al., 2003; Heitzman et al., 2007; Dickmann and Leefers, 2006). These forests were originally dominated by *Quercus* spp. and *Carya* spp., leading European botanical explorers to think that the *Quercus*–*Carya* association was one of only a few climax types in Eastern North America. Subsequent thinking and observations have led to a different picture. Apparently, most of these forests were maintained by regular fires—either intentionally set by Native Americans for hunting or escaped from Native American agricultural activities—repeatedly clearing any non-fire tolerant species and leaving the *Quercus* and *Carya* species and the few other species that cohabited with them. Upon the establishment of fire-control regimes in these forests, the *Quercus* and *Carya* were unable to establish new recruits in the understory due, presumably, to the heavy competition of the other species that were now prospering due to the control of fires. In this case these species are *Acer rubrum* (Red Maple), *Prunus serotina* (Black Cherry), and *Hamamelis virginiana* (Witch Hazel). Since the fires came under control only approximately 100 years ago (Dickmann and Leefers, 2006), this new understory com-

munity has had only a short period of time to establish itself. The pattern they form in the understory is dramatically non-random, and is, largely, the subject of this thesis.

The forest in question is located at the ES George Reserve near Pinckney, MI Livingston County. The forest is in a section of the reserve that has had complete forest cover since at least 1940 (from aerial photographic documentation see Figure 6.1). Within this forested area a permanent plot, called the Big Woods Plot, of 22ha was established in 2003, all trees greater than 10cm girth at breast height (GBH) were tagged, identified and georeferenced within the plot. With the exception of one purely theoretical chapter, this thesis is based on empirical evidence from this plot.

I examine (1), how pattern is formed, in the first three chapters: In Chapter II I provide evidence for a system in which biological interactions give rise to spatial pattern in a homogenous environment. This theoretical result is a discrete-time and discrete-space version of Turing's diffusive instabilities. It is biologically motivated by the idea of two different types of competition—reproductive and resource—and these two acting at different scales.

For a specific example of ecological interactions causing spatial pattern I examine *Hamamelis virginiana*, which exhibits a striking spatial pattern in the understory of our plot (Figure 3.1). In chapter III I provide evidence that this pattern arises from the interaction of dispersal limitation—*H. virginiana* disperses through short-distance mechanical dehiscence—and Janzen–Connell, density-dependent seed mortality due to a small curculionid seed predator, *Pseudanthonomus helvolus*. I propose that new *H. virginiana* patches start from rare long-distance dispersal events; expand locally from the typical short-distance dispersal; and then once the patches reach a certain size they attract the seed predator, recruitment slows, and the patches thins or dies.

In the next Chapter, IV, I expand the ideas introduced in chapter III to the other dominant understory species, *P. serotina* and *A. rubrum*. That is I demonstrate that

the spatial pattern observed in the understory of the Big Woods plot could arise through the ecological interactions of these three main species—specifically through the combination of the history of the forest, dispersal limitation, and Janzen–Connell seed and seedling mortality. I then incorporate these ecological interactions into a stage-structured, spatially explicit model which, upon instantiation from field data, reproduces qualitatively similar patterns to those observed.

To examine (2) I run the model for chapter IV forward from the given current spatial distribution. This gives some indication about what the forest will look like in the future. We know that the current overstory species of *Quercus* and *Carya* will be replaced, in the medium term, by *P. serotina* and *A. rubrum*. This model examines how the current spatial distribution of these species will affect the successional pattern of the forest. Particularly how their jigsaw-like spatial pattern affects their competition together, and whether this jigsaw pattern will persist into the overstory as these species become the major component of it. This is also covered in Chapter IV.

Exclusive of the relationship between ecological interactions and pattern formation, the Big Woods Plot gives insights into similar northeastern North American forests that are undergoing such a dramatic shift in composition. The final two chapters examine two such insights. Chapter V elaborates a method for determining the successional state of a forest, using the popular metabolic theory of ecology. This metabolic theory predicts a power-law distribution of trunk sizes within a forest stand (West et al., 2009). In this forest I find a systematic deviation from this distribution, with too many large trees and that all of these trees are *Quercus* and *Carya*.

In Chapter VI I examine whether some swamp hummocks next to the forest function, biologically, as islands in regard to the forest tree flora. The islands farthest from the forest mainland have fewer species than patches of the forest of an equal size, but this is true just of "new" species. That is species that we assume have re-

cently increased their number due to fire suppression are under-represented on those hummocks farthest from the mainland. This supports our understanding of the successional history of the forest, because these species would have had the shortest time to emigrate to the farthest islands.

# CHAPTER II

# Extensions in space destabilizes an otherwise stable coupled-map lattice

## 2.1 Introduction

Turing (1952) devised a system of differential equations with a locally stable solution, which when extended spatially with a reaction-diffusion equation formulation became unstable, leading to characteristic spatial patterning. Turing's insight provided a counter-intuitive mechanism by which non-random patterns can form in a homogenous environment in which the interacting particles diffuse randomly. Increasingly ecologists are suggesting that this mechanism may play a role in pattern formation in some ecological systems (Klausmeier, 1999; Rietkerk et al., 2004*b*; van de Koppel et al., 2005). Concurrently there has been an increase in theoretical work relating to the Turing mechanism, ultimately resulting in a complete analysis of the mathematical conditions for an $n$-equation reaction diffusion system to have Turing instability (Satnoianu et al., 2000).

All of these empirical and theoretical studies have continued Turing's convention of looking at the problem in the reaction-diffusion (i.e., continuous-time and continuous-space) context. But there is no inherent reason this process could not take place in a discrete-space and discrete-time context. In fact Hastings (1992) and

Doebeli and Killingback (2003) present coupled-map lattices (discrete-space discrete-time analogues to reaction-diffusion equations) which do just that and connect their work to Turing. But as of yet there has been no systematic attempt to find the mathematical conditions for coupled-map lattices to have Turing instability, as Satnoianu et al. (2000) did for reaction-diffusion equations. There is no *a priori* reason to think the conditions will be similar, since very simple models may have qualitatively distinct outcomes depending on whether they are formulated in a discrete or continuous context (Durrett and Levin, 1994).

In this note we seek to begin this investigation. We present a model that is structurally similar to that of Bascompte and Solé (1994) and Rohani et al. (1996), with the exception that we distinguish migratory effects on reproduction from migratory effects on intraspecific competition, or, equivalently, effects on reproduction and survivorship. Biologically our approach is similar to that of Doebeli and Killingback (2003) and Hastings (1992), but with a mathematical form that is considerably less complicated.

Suppose that lattice points are coupled with two distinct rules, associated with two distinct population parameters, reproduction and intraspecific competition (or, equivalently, density dependence). So, for example, the dispersion of seeds (reproductive coupling) may be distinct from root competition (density-dependent coupling), wherein we imagine the overall population density at a neighbor lattice point contributes some fraction of its biomass to reproduction, but only half (say) of that population density has roots that grow to influence the process of below-ground competition (Doebeli and Killingback, 2003). Or, early migrants of an annual species contribute to reproduction, but later migrants arrive after the reproductive season has ended. Or, different life stages migrate, only some of which have reached adulthood (and thus can reproduce) while all contribute to the utilization of resources and thus contribute to the general density dependent effect (Hastings, 1992). Other

biological configurations are easy to conger.

One way of conceptualizing this phenomenon is with dual, potentially incommensurate, coupling coefficients. Thus, if $N_{i,j}(t)$ is the population size at lattice point $i, j$ at time $t$, we consider the following model:

$$N_{i,j}(t+1) = r(N_{i,j}(t) - m_1 N_{i,j}(t) + m_1 \overline{N_{i,j}(t)}) f(N_{i,j}(t) - m_2 N_{i,j}(t) + m_2 \overline{N_{i,j}(t)}). \quad (2.1)$$

Where $r$ represents the maximum rate of population growth, $m_1$ and $m_2$ represent the reproductive and intraspecific-competition migration, respectively. The function $f(N)$ represents the density dependence of population growth within each patch and $\overline{N_{i,j}(t)}$ is the average population in the patches that disperse into the $i, j$ patch. An analysis of the spatially homogenous equilibrium solution is presented in Appendix 1. Here we proceed with a specific example.

## 2.2 An Example

We assume a one-dimensional circular (periodic boundary conditions) array of $n$ patches in which each population migrates into the two adjacent patches and the density dependence is given by a simple linear function, $f(N) = 1 - N$. (These assumptions simplify the analysis, but as shown in Appendix 1, the results are robust for a two-dimensional array of patches and other forms of density dependence.) This gives rise to the model:

$$N_i(t+1) = r(N_i(t) + m_1(0.5(N_{i+1}(t) + N_{i-1}(t)) - N_i(t)) f(N_i(t) + m_2(0.5(N_{i+1}(t) + N_{i-1}(t)) - N_i(t))). \quad (2.2)$$

This set of $n$ difference equations has an equilibrium solution of $N_i^* = 1 - \frac{1}{r}$. This corresponds to a spatially homogenous equilibrium where the population at each patch is the same as it would be in the non-spatial logistic model.

Linearizing about this equilibrium solution yields the Jacobean matrix:

$$J = \begin{pmatrix} a & b & 0 & \cdots & & & 0 & b \\ b & a & b & 0 & \cdots & & & 0 \\ 0 & b & a & b & 0 & \cdots & & 0 \\ & & \ddots & \ddots & \ddots & & & \\ 0 & \cdots & & & 0 & b & a & b \\ b & 0 & \cdots & & & 0 & b & a \end{pmatrix}. \tag{2.3}$$

Where $a = 2 - r - (m_1 + m_2 - rm_2)$ and $b = 0.5(m_1 + m_2 - rm_2)$. The eigenvalues of matrices of this form are $\lambda_k = a + 2b\cos(\frac{2\pi k}{n})$ with $k = 0, 1, \cdots, n-1$ (May, 1974). The spatially homogenous equilibrium is unstable if any of these is greater than one in absolute value. Notice that $\lambda_0 = 2 - r$, so the equilibrium is unstable if $r > 3$—just like in the non-spatial logistic model. So this model predicts, as have others (Rohani et al., 1996), that metapopulation dynamics cannot stabilize systems that would be unstable in non-spatial models. (Although increasing migration will cause the absolute value of most of the eigenvalues to be less than one and when the model is simulated oscillations are damped when compared to the non-spatial model for a very long transient period before they reach non-spatial levels.)

On the other hand this equilibrium can be unstable for values of $r$ which would lead to stable behavior in the non-spatial model. Since only one eigenvalue must be larger than one in absolute value for instability we consider the eigenvalue most affected by migration. If $n$ is even consider $\lambda_{\frac{n}{2}} = a - 2b$ and if $n$ is odd consider $\lambda_{\frac{n+1}{2}} = a - 2b\cos(\frac{\pi}{n})$, which in the limit of large $n$ is also $a - 2b$. In either case we have an eigenvalue close to $2 - r - 2(m_1 + m_2 - rm_2)$. So the equilibrium is unstable if $r + 2(m_1 + m_2 - rm_2) > 3$. Thus the spatially homogenous equilibrium can be unstable for values of $r$ which would predict stability in the non-spatial model.

The destabilization of the spatially homogenous equilibrium leads to interesting

temporal and spatial dynamics. Simulations on a two-dimensional grid reveal that if the conditions are met to destabilize the spatially homogenous equilibrium then individual patches cycle out of phase with their neighbors. At any particular time the grid has a checkerboard-like structure (Figure 2.1), and through time individual patches exhibit a two-cycle. Also if we simulate this model with values of $r$ that generate two cycles in the non-spatial logistic model we find another interesting result. When coupling patches with only intraspecific-competition migration, all patches reach the same population value and cycle in phase. Contrarily, coupling the patches only by reproductive migration, a rich spatial structure emerges in which a subset of the patches cycle in phase with each other and out of phase with the remaining patches (Figure 2.2). Thus the frequently asserted assumption that oscillating patches in a metapopulation become in phase with each other due to migration is an oversimplification (Earn et al., 2000).

For this effective phase reversal it is necessary that $m_1 > m_2$, which is to say, reproductive migration must be of more importance than intraspecific-competition migration. When Vandermeer and Kaufmann (1998) coupled two logistic maps with either reproductive or intraspecific-competition migration they found that increased reproductive migration decreased the basin entrainment of the two maps while increasing density migration increased the basin of entrainment. Our results can at least partially be explained by this mechanism, since reproductive migration tends to decrease the likelihood that two neighbors become entrained, thus disrupting any tendency towards the spatially homogenous equilibrium. Intraspecific-competition migration has the opposite effect.

Hastings (1992) observed this trend in a model in which he explicitly modeled different migration rates for different age classes within a metapopulation setting. He notes that when the strongly density-dependent age classes are stationary ($m_2 = 0$ in our case) it is possible for the spatially homogenous equilibrium to be destabilized

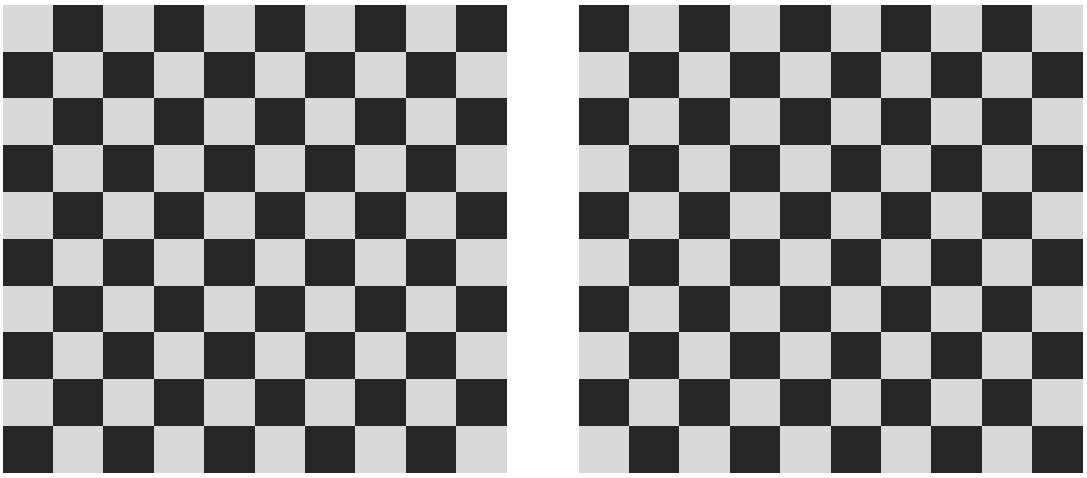

Figure 2.1: Consecutive time steps from equation 2.1 iterated on a 9-by-9 grid with $f(N) = 1 - N$, $r = 2.9$, and $m_1 = 0.1$ and $m_2 = 0.01$. The gray-scale represents the population density at each site on the grid. A stable equilibrium is not reached, as would be expected in a logistic equation with this $r$ value. Instead each site displays a two-cycle out of phase with its neighbors.

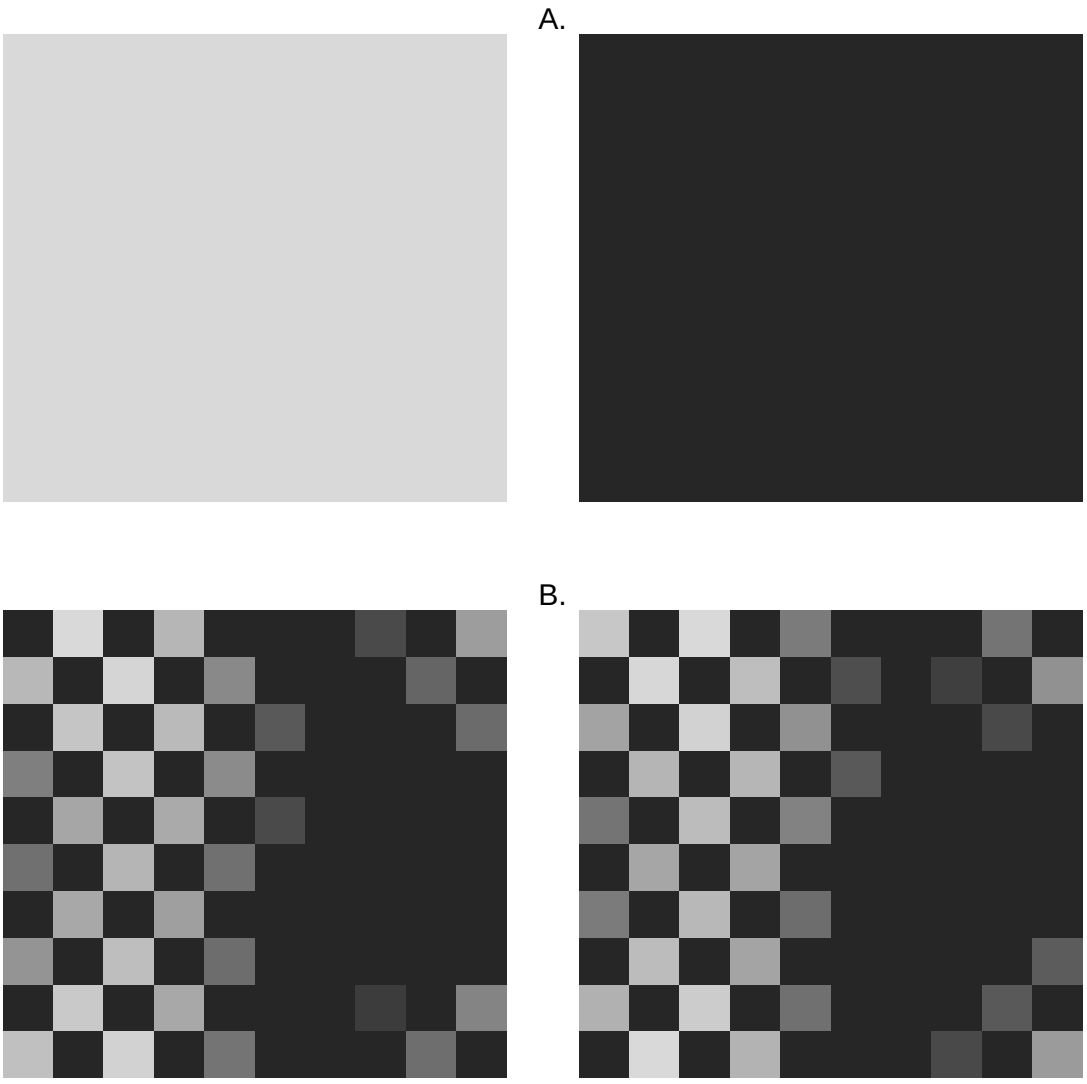


Figure 2.2: Consecutive time steps from equation 2.1 iterated on a 9-by-9 grid with $f(N) = 1 - N$, $r = 3.1$ after transient behavior. A. Shows the array in two consecutive time steps with $m_1 = 0$ and $m_2 = 0.1$. B. the array in two consecutive time steps with $m_1 = 0.1$ and $m_2 = 0$. In each case the gray-scale represents the population density at each site on the grid.

when it would be stable in the non-spatial case. Interestingly our results are in disagreement with the work of Doebeli and Killingback (2003) who find that in the absence of dispersal, quasi-local competition, which is analogous to our intraspecific-competition migration, destabilizes what would be a stable equilibrium in a non-spatial setting. We show in Appendix 2 that contradiction results from a slight difference in the way their model is constructed.

## 2.3 Appendix 1

Here we examine the stability of the homogenous equilibrium solution to equation 2.1. First consider the general non-spatial model. We have $N(t+1) = rN(t)f(N(t))$ where $r$ is the maximum growth rate and $f(N)$ describes the density dependence. If we have an equilibrium, $N^*$, then it will satisfy $f(N^*) = \frac{1}{r}$ . This equilibrium is stable if and only if $|1 + rN^*f'(N^*)| < 1$. Let $rN^*f'(N^*) = R$. Note that since $f'(N^*) < 0$ we will have $R < 0$. Thus instability can only occur if $R < -2$.

Now we can consider our general model (equation 2.1) on a two-dimensional grid of $n^2$ patches. We assume periodic-boundary conditions (torus) and that each patch sends migrants into its Von Neumann neighborhood. Again we shall consider the stability of the spatially homogenous equilibrium solution, where the population at all patches is $N^*$ and $f'(N^*) = \frac{1}{r}$.

Again in order to determine the stability of this equilibrium we linerarize about this solution. This yields an $n^2$-by-$n^2$ matrix, $J$, of the same form described in Rohani

et al. (1996),

$$J = \begin{pmatrix} J_1 & J_2 & J_3 & \cdots & & & J_3 & J_2 \\ J_2 & J_1 & J_2 & J_3 & \cdots & & & J_3 \\ J_3 & J_2 & J_1 & J_2 & J_3 & \cdots & & J_3 \\ & & \ddots & \ddots & \ddots & & & \\ J_3 & \cdots & & & J_3 & J_2 & J_1 & J_2 \\ J_2 & J_3 & \cdots & & & J_3 & J_2 & J_1 \end{pmatrix}. \tag{2.4}$$

Where $J_1$, $J_2$, and $J_3$ are $n$-by-$n$ matrices. With

$$J_1 = \begin{pmatrix} a & b & 0 & \cdots & & & 0 & b \\ b & a & b & 0 & \cdots & & & 0 \\ 0 & b & a & b & 0 & \cdots & & 0 \\ & & \ddots & \ddots & \ddots & & & \\ 0 & \cdots & & & 0 & b & a & b \\ b & 0 & \cdots & & & 0 & b & a \end{pmatrix}; \tag{2.5}$$

$J_2 = bI$ (where $I$ is the identity matrix); and $J_3$ is a matrix of zeros. Here $a = 1+R-(m_1+Rm_2)$ and $b = 0.25(m_1+Rm_2)$. Again from May (1974) the eigenvalues of this matrix are $\lambda_k = a + 2b[\cos(\frac{2\pi k}{n}) + \cos(\frac{2\pi k}{n^2})]$ where $k = 0, 1, \cdots, n^2-1$. As in Rohani et al. (1996) we can choose a $k \approx \frac{n^2}{2}$, such that $\cos(\frac{2\pi k}{n}) + cos(\frac{2\pi k}{n^2}) = -2$ in the limit of large $n$. So we have an eigenvalue close to $a-4b = 1+R-2(m_1+Rm_2)$.

As $R$ is negative we have instability if $-2 > R-2(m_1+Rm_2)$. Recall from above the condition for instability in the non-spatial model $-2 > R$. Thus our conclusions from the specific model—that spatial dynamics can destabilize systems which would be stable in the non-spatial case and that $m_1$ must be large compared to $m_2$ for this to happen—also hold for a two dimensional array of patches and for any from of density dependence.

## 2.4 Appendix 2

Consider Doebeli and Killingback's (2003) model,

$$N_{t+1} = \frac{\lambda}{1 + a[N_i(t) + \alpha(N_{i-1}(t) + N_{i+1}(t))]} \tag{2.6}$$

where $\alpha$ is the level of quasi-local competition, which is analogous to $m_2$. As $\alpha$ increases each site feels an increase in competitive effect from its neighbor's populations and its population increases its competitive effect on its neighbors, but this does not result in a decrease in the competitive effect an individual site feels from its own population. This is not the case in our model from equation 2.1. We show here this difference is responsible for the different predictions of the two models.

Consider again a one-dimensional circular array of $n$ populations. To simplify analysis and for the ease of comparison, we connect these populations only with quasi-local competition (or equivalently intraspecific-competition migration). This gives rise to the model,

$$N_i(t+1) = rN_i(t)f((1 - m_2')N_i(t) + \frac{m_2}{2}(N_{i+1}(t) + N_{i-1}(t))). \tag{2.7}$$

Here $m_2$ is the amount of intraspecific-competition migration and $m_2'$ is the amount this migration reduces the competitive effect of individuals on their original patch. So if $m_2' = m_2$ we recover our original model and if $m_2' = 0$ we have Doebeli and Killingback's (2003) formulation.

Performing the same stability analysis on a spatially homogenous equilibrium as above we have eigenvalues, $a + 2b\cos(\frac{2\pi k}{n})$, where $a = 1 + R - 2Rm_2'$, $b = Rm_2$, and $k = 0, 1, \cdots, n-1$. When $k = 0$ we have the eigenvalue $1 + R + 2R(m_2 - m_2')$. When $m_2' = m_2$ as previously shown in our model the eigenvalue is just $1 + R$ as in the non-spatial case and intraspecific competition migration cannot destabilize the

equilibrium. But if $m_2' = 0$ we have an eigenvalue of $1+R+2Rm_2$ which could be less than $-1$, even if $1+R$ is not. Thus destabilizing the spatially homogenous equilibrium as in Doebeli and Killingback (2003). This simple general model is able to recover their prediction and illustrates the cause of the apparent contradiction between our results.

# CHAPTER III

# Dispersal limitation and Janzen–Connell effect lead to spatial pattern in a *Hamamelis virginiana* stand

## 3.1 Introduction

The spatial distribution of individuals within a population is of increasing interest to ecologists. Historically it was assumed that observed nonrandom patterns in these distributions were largely the result of underlying environmental heterogeneity. However there has long been theoretical evidence of the possibility for endogenous pattern formation in the absence of underlying exogenous spatial heterogeneity (Turing, 1952). Increasingly this idea has been applied in ecological systems (Bascompte and Solé, 1994; Kéfi et al., 2007; Klausmeier, 1999; Pascual, 1999; Perfecto and Vandermeer, 2008; Rietkerk et al., 2002; Solé and Manrubia, 1995; van de Koppel et al., 2005). The expanding series of 50ha forest plots offers a wealth of data to study spatial patterns in ecological systems, and has made it clear that many species within the plots are highly spatially aggregated (Condit et al., 2000). Although some species' aggregation correlates with underlying environmental conditions (Engelbrecht et al., 2007), many species show no evident correlations with any environmental variables. This suggests that the aggregation may result from some endogenous process.

Furthermore the level of aggregation is dependent on the mode of seed dispersal, with mechanically dispersed species the most aggregated, then wind-dispersed species, and then animal-dispersed species (Seidler and Plotkin, 2006). This aggregation persists in the face of, most likely, strong Janzen–Connell pressure, which was initially assumed to lead to a non-aggregated, uniform distribution of trees (Janzen, 1970; Connell, 1971, 1978). In order to truly understand how these endogenously generated distributions arise we must understand the seemingly counteractive forces of dispersal limitation and Janzen–Connell recruitment limitation. Although much of the literature examines these questions in the tropics, the problem may be more tractable in the temperate region, where the much lower diversity of tree species may make the patterns much more evident.

*Hamamelis virginiana* in the understory of the Big Woods plot at the E.S. George Reserve in Pinckney, MI offers are particularly distinct spatial pattern (Figure 3.1). In the understory of this forest *H. virginiana*, *Prunus serotina*, and *Acer rubrum* form a tight mosaic (Figure 4.1). The pattern of the three species together is examined in Chapter IV, but here I consider *H. virginiana* alone because its pattern is the tightest and most clear.

*H. virginiana* has short-distance, mechanical dispersal—ejecting seeds as the fruits dehisce . Anderson and Hill (2002) measured 45 dispersed seeds and found an average distance of 3.45m and none of the seeds dispersed beyond 5m. Thus we would expect that *H. virginiana* should be very aggregated. But, at the same time, *H. virginiana* seeds are parasitized by an obligate seed parasite, *Pseudanthonomus helvolus*, which can parasitize as many as 90% of the non-aborted fruits (De Steven, 1981, 1982, 1983*b*; Clark, 1987) and could exert a strong density-dependent, Janzen–Connell recruitment limitation. In fact De Steven (1983*b*) found that furits on small, isolated *H. virginiana* individuals were slightly less likely to be parasitized by *P. helvolus*. But De Steven (1983*b*) did not have a complete map of *H. virginiana* individuals in her study area—

also the ES George Reserve—and thus could find few isolated individuals and used nearest neighbor distance, not local density, to quantify isolation. With the complete map of *H. virginiana* individuals we can better address this question. As such the species offers a great opportunity to examine the counteractive forces of dispersal limitation and Janzen–Connell recruitment limitation.

Here I examine the effect of these two forces on *H. virginiana* in an area where it shows significant spatial aggregation. We find significant evidence of Janzen–Connell seed parasitism, with large clumps of *H. virginiana* experiencing more parasitism than isolated individuals or those in small clumps. From these two forces, dispersal limitation and density-dependent recruitment limitation, we create a phenomenological model of patch demography which is broadly consistent with the spatial pattern observed. This model is made explicit and incorporated with the other understory species in Chapter IV.

## 3.2 Methods

This study was conducted at the E.S. George Reserve in Pinckney, MI. This site has a 22ha plot in which all stems larger than 10cm GBH are identified, measured and spatially referenced. Twelve hectares were originally censused in 2003 and re-censused in 2008. The other ten hectares have been added since then, though only censused once. For more details on the site and census technique see Jedlicka and Vandermeer (2004), and for a thorough discussion of the forest structure see Section 4.2.

To study the *H. virginiana* pattern we defined a number of *H. virginiana* "clumps." We say two individuals are in the same clump if they are within 10m of each other. The plot has 3046 *H. virginiana* individuals larger than 10cm GBH distributed between 18 clumps and a handful of "isolated" individuals (Figure 3.1). *H. virginiana* has vegetive reproduction through suckers. This forms multi-stem trees, which were counted as a

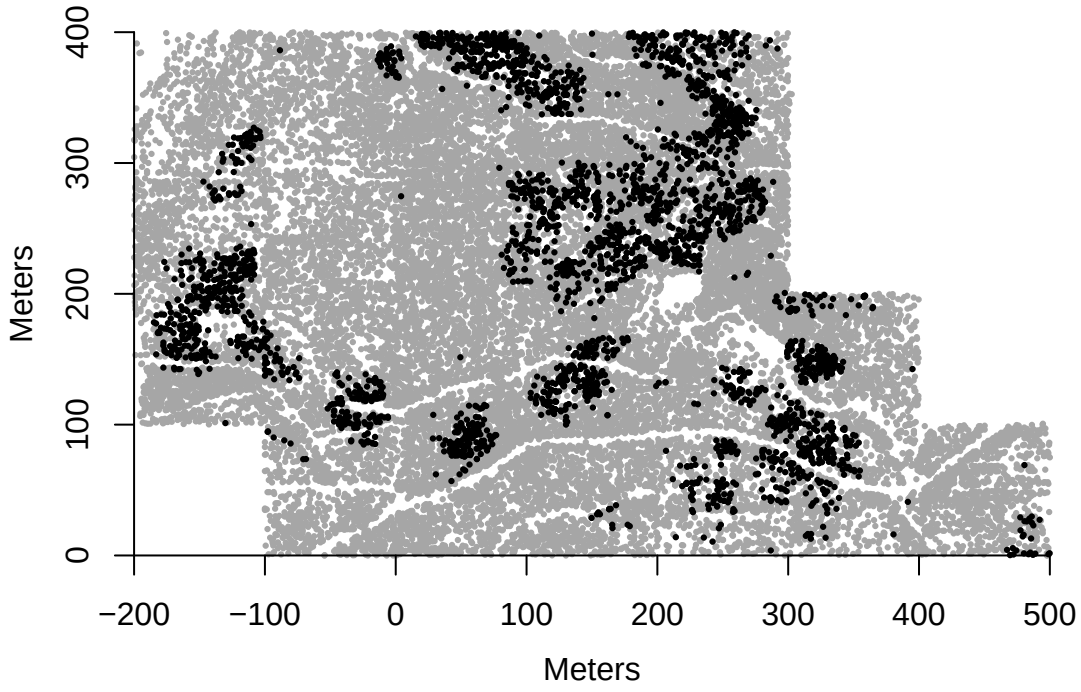


Figure 3.1: Distribution of *H. virgiana* stems individuals within the Big Woods Plot. The light gray dots are all trees—to show the extent of the plot—and the black dots are the *H. virgiana* individuals. They are significantly clustered at a range of scales (Figure 3.2).

single individual in our surveys.

*H. virginiana* flowers and is pollinated in late fall, but the pollen tube grows only halfway down the style and overwinters in that stage. The pollen tube grows the rest of the way in April, followed by fertilization and fruit set (De Steven, 1983*a*). The fruit, which contains two seeds, develops on the tree until late September–early October when the fruit dehisces and disperses the seeds. During this long development period the fruit are eaten by lepidopteran larvae and chipmunks (De Steven, 1982). The fruit are also parasitized by an obligate seed parasite, *P. helvolus* (De Steven, 1982, 1983*b*; Clark, 1987).

In May of 2008, at the time of fruit set, we tagged twenty fruits on each of ten *H. virginiana* trees (1) within each of eight clumps and (2) on ten isolated trees (for a total of 1800 tagged fruits). *P. helvolus* oviposition marks are distinctive, and the larvae can then eat one or both of the developing seeds or be parasitized by one of a number of parasitic wasps (De Steven, 1981). Lepidopteran larvae and chipmunks also feed on *h. virginiana* fruits, and their feedings is distinctive. Prior to seed dispersal, in September, we removed and dissected the fruit to determine how many viable seeds were left and the fate of the *P. helvolus* larvae. We also collected litter samples ($1m^2$ samples) in the fall of 2009 in the various clusters of *H. virginiana* and paired these with litter samples outside of those clusters. From these samples we extracted the weevils using mini-Winkler extractors (Fisher, 1999; Besuchet et al., 1987).

## 3.3 Results

*H. virginiana* stems exhibit a strongly nonrandom aggregated spatial pattern (Figure 3.1). They are significantly more clustered than expected due to random at all spatial scales from 0m to 25m (Figure 3.2). These clumps show a strong age structure, with larger clumps having significantly larger, and presumably older, individuals then smaller clumps (Figure 3.3). Over the five years between surveys there was a trend for

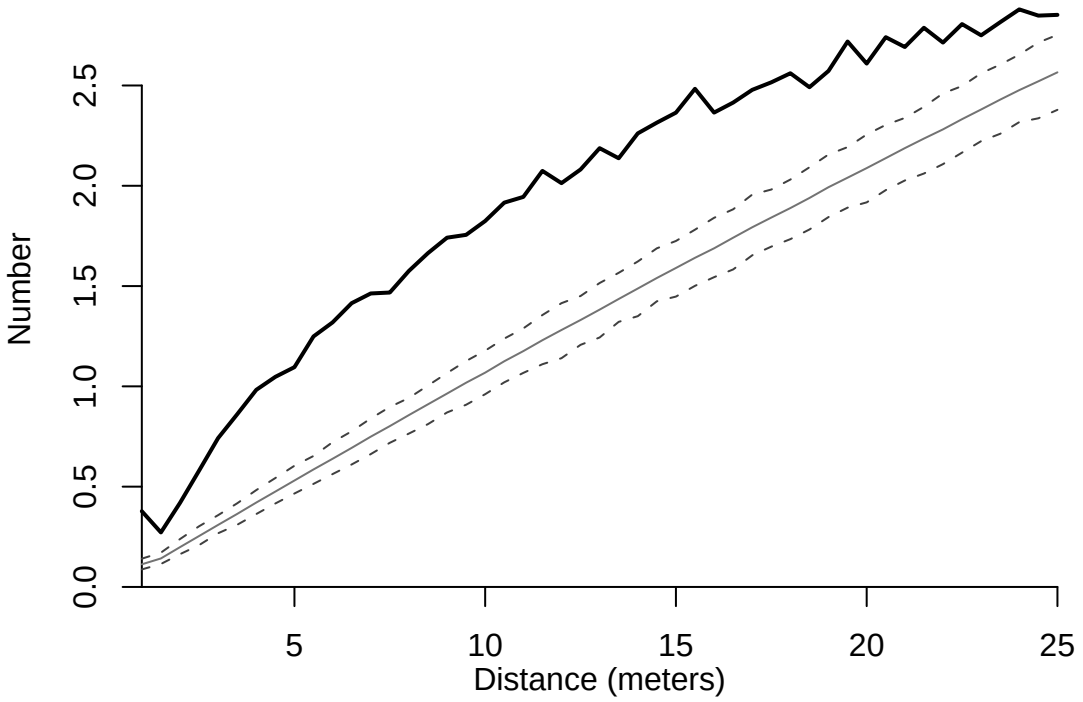


Figure 3.2: Average number of *H. virginiana* found within 0.5-meter wide "donuts" a given distance around other *H. virginiana*. The black line is the observed value and the gray the expectation if the *H. virginiana* individuals were distributed randomly and the dotted lines are the 95% confidence limits around the expectation.

the larger clumps to decrease in number of stems, while the smaller clumps increased in number of stems (Figure 3.4). All of these observations are more consistent with the patches being endogenously formed and dynamic, rather than the result of some underlying habitat heterogeneity.

There was significant variation in the number of fruits parasitized by *P. helvolus*. After initial fruit set a large proportion of fruits are aborted, before the emergence of the adult weevil. Thus we examined the proportion of non-aborted fruits that are parasitized. Seeds in non-aborted fruits survived at a higher rate on isolated *H. virginiana* and on those in smaller patches than in larger patches (Figure 3.5). There was no such trend for chipmunk or lepidopteran damage, which were unaffected by

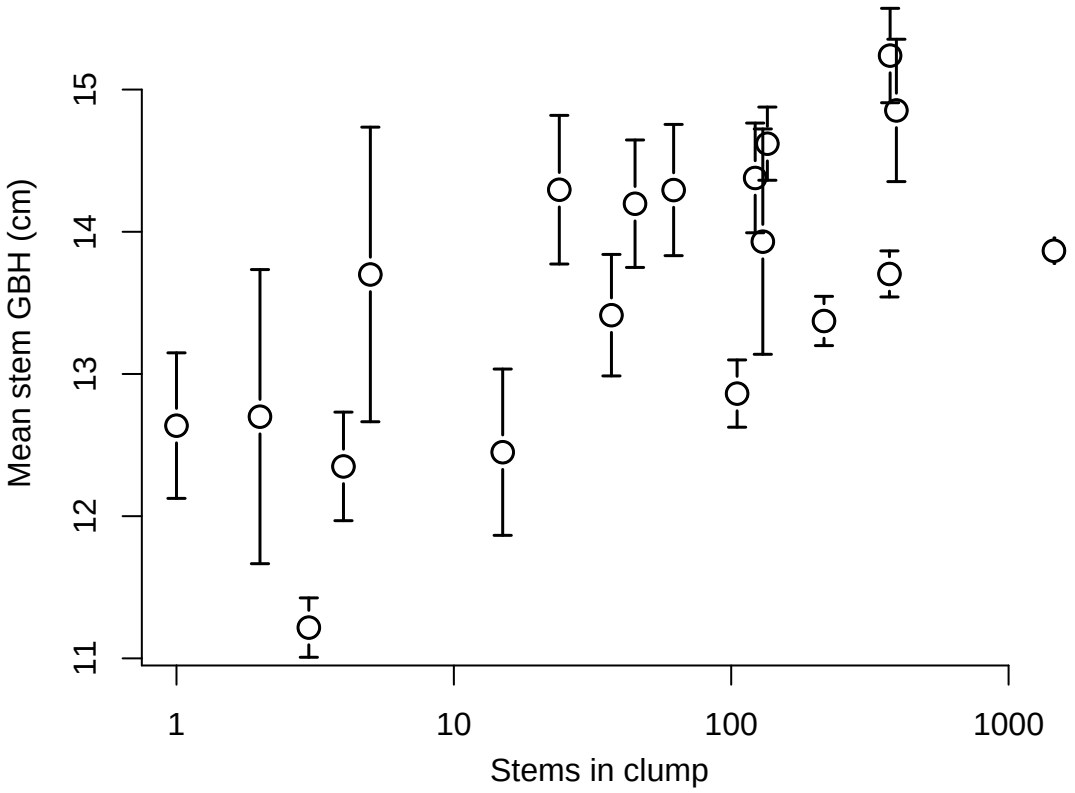


Figure 3.3: Average girth at breast height (GBH) of a stem in a clump versus the number of stems in that clump. Standard errors indicated. There is a clear relationship, with large clumps having larger trees and small clumps smaller trees.

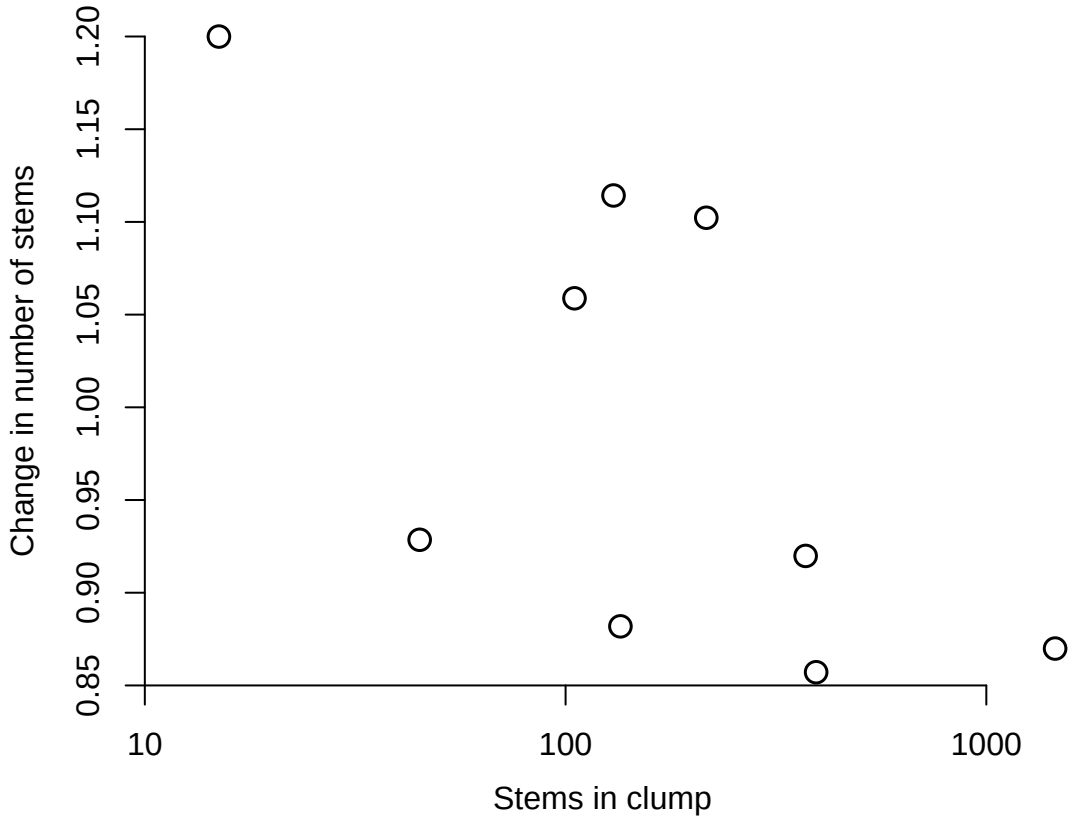


Figure 3.4: Proportion change in the number of stems in a clump between 2003 and 2008 versus the number of stems in that clump. The larger clumps now have fewer stems, while the smaller have more.

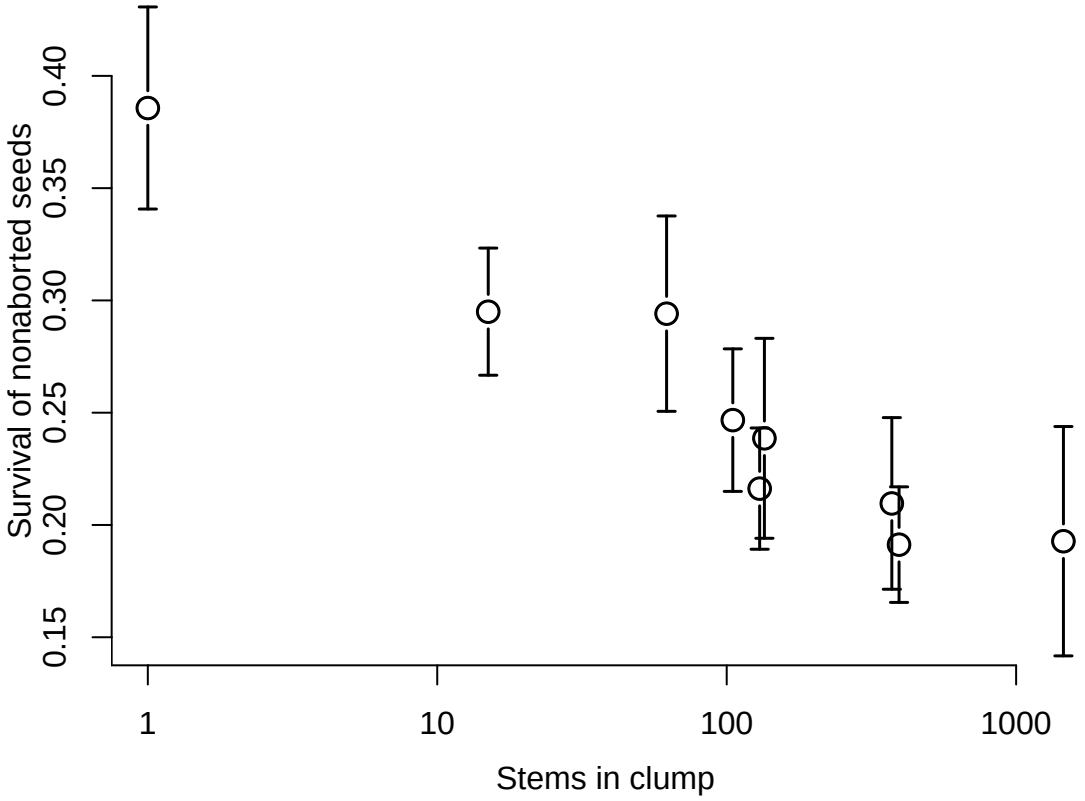


Figure 3.5: Proporiton of nonaborted *H. virginia* seeds that survived versus number of stems in clump. Standard errors indicated.

local *H. virginiana* density and accounted for very little seed mortality. Furthermore, the litter samples revealed a higher population density of beetles within clusters of *H. virginiana* (0.77 beetles per sample with ± 0.19 standard error) compared to zero found in paired sites outside of clusters.

## 3.4 Discussion

Here we find evidence for the Janzen–Connell effect by seed predation by *P. helvolus* on *H.virginia*. As *H. virginia* patches increase in size they experience increased seed parasitism, consistent with the Janzen–Connell effect. This effect has generally been assumed to be mostly a tropical phenomenon, but there is some evidence of

its impact in the temperate region. Hille Ris Lambers et al. (2002) found density-dependent seed and seedling mortality for a number of temperate tree species; Packer and Clay (2000, 2003) found lower *Prunus serotina* recruitment and lower seedling growth and survival around adult *P. serotina*; and De Steven (1983*b*) found an indication that isolated *H. virginiana* trees had a lower rate of fruit parasitism. Here we were able to expand on De Steven (1983*b*) results because we had a complete spatial census of the *H. virginiana* in the area. The Janzen–Connell effect in this case is not entirely surprising because *P. helvolus* is an obligate predator, has limited mobility, and *H. virginiana* builds up dense clumps of its hosts.

What is more surprising is that even in the face of strong Janzen–Connell pressure the spatial distribution of plants can be highly aggregated. Further, these results suggest that the role of the Janzen–Connell effect could be in constraining fecundity of individuals in larger clumps—thereby limiting clump size—rather than preventing clumps from forming in the first place. Thus aggregated distributions observed in many plant communities may not be, in and of themselves, evidence of the absence of the Janzen–Connell effect.

Further we propose that the spatial pattern of *H. virginia* is due to a self-organized pattern of local expansion due to dispersal limitation, and then patches slowing growth or contracting due to some regional density-dependent mechanism. We think that this mechanism is density-dependent seed mortality effect of *P. helvolus*, but we cannot distinguish it from self thinning independent of weevil seed predation. Although we cannot resolve the mechanism completely we do have support for this heuristic model of patch demography. The size of *H. virginiana* individuals—and thus most likely age—within a patch correlated with the size of that patch, as would be predicted if the patches arose through a self-organized process and not as a result of underlying environmental heterogeneity. Further larger patches lost stems over the five years, while smaller patches gained.

Put together, these results suggest a mechanism for self-organized spatial pattern formation that could be seen in many plant species; dispersal limitation causes an initial aggregated distribution of plants, and then some density-dependent mortality (like the Janzen–Connell effect) causes the growth of these clumps to slow or stop. The mechanism is, phenomenologically, very similar to that proposed by Turing (1952) of an activator and an inhibitor when he originally demonstrated the possibility for self-organized pattern formation. Here the activator is seed dispersal itself and the inhibitor is the predator/herbivore involved in the Janzen–Connell effect. It is also phenomenologically similar to that described in other systems (Perfecto and Vandermeer, 2008). Consequently, we might expect, in many systems the scale of aggregation will be determined by the scale of dispersal (closely tied to the mode of dispersal) coupled with the intensity and scale of the Janzen–Connell effect.

# CHAPTER IV

# Janzen–Connell in the temperate zone: contribution to pattern formation in a successional forest

## 4.1 Introduction

Ecosystems rarely exhibit random spatial patterns. Acknowledging this fact animates a huge literature on the nature and causes of non-randomness (Solé and Manrubia, 1995; Klausmeier, 1999; Pascual et al., 2002; Rietkerk et al., 2002). An early insight into what could be a major determinant of spatial pattern emerged from detailed study of recruitment in tropical trees by Janzen, an effect subsequently known throughout the literature as the Janzen–Connell effect (Janzen, 1970; Connell, 1971, 1978). A completely separate literature, mainly in theoretical ecology, has focused on the idea that ecological rules operative at a local scale may translate into emergent pattern at a regional scale, effectively a case of self-organized pattern (Solé and Manrubia, 1995; Klausmeier, 1999; Pascual et al., 2002; Rietkerk et al., 2002). A moment's reflection reveals the obvious fact that the Janzen–Connell effect could provide a mechanism, operating at a local level, for the emergent pattern at a much larger scale. Although some connections between the Janzen–Connell effect and spatial patterns have been made (Augspurger, 1984; Clark and Clark, 1984; Howe, 1989; Wills

et al., 2006), its general role in emergent pattern formation has largely escaped the attention of ecologists. This is, perhaps, because consideration of the Janzen–Connell effect has been almost exclusively in tropical regions, where high species diversity renders the existence of large-scale pattern difficult to observe.

Temperate zone forests, with their relatively low species diversity, thus emerge as ecosystems in which these dynamics might be more easily observed. Reports of the Janzen–Connell effect in temperate forests (De Steven, 1983*b*, 1982; Packer and Clay, 2000; Hille Ris Lambers et al., 2002) are rare compared to the tropical literature. This may be because ecologists are less interested investigating the Janzen–Connell effect there since explaining alpha diversity in temperate forests is not a major goal, as it is in tropical forests. Here we report on two clear cases of its operation and discuss how their operation at a local level creates a distinct pattern in three species of subcanopy trees in a forest that is undergoing succession from *Quercus*-dominated to *Acer rubrum*-dominated canopy.

Many forests in northeastern North America are undergoing a dramatic decline in the proportion of *Quercus* and *Carya* species in the canopy(Zhang et al., 2000; Heitzman et al., 2007; McDonald et al., 2003). Often concurrent is an increase in the canopy proportion of *Acer rubrum*, this process is thus known as the "Red Maple Paradox" (Abrams, 1998, 1992), and has been underway for perhaps as much as a century. Given this relatively recent initiation of the process, it is possible to tease out several dynamic aspects of the forest by looking at size and location variables. Here we focus on a case of dramatic spatial structure, the causes of which are deducible if we take into account the history of the forest coupled with two cases of the Janzen–Connell effect.

The area in question is a transitional forest in which the *Quercus–Carya* overstory is being slowly replaced by *A. rubrum* and *Prunus serotina*, both of which currently share subcanopy dominance with *Hamamelis virginiana*. Ultimately these species will

be replaced by others— *Acer saccharum*, *Fagus grandifolia*—but in the medium term *A. rubrum* and *Prunus serotina* will dominate the canopy as the *Quercus* and *Carya* die. The abundance and distribution of these three species are assumed to be the result of fire suppression initiated by European settlers in the latter part of the nineteenth century (Dickmann and Leefers, 2006), which has resulted in a mosaic spatial pattern in the forest's understory (Figure 4.1). We propose this distinctive mosaic structure results from 1) expansion from focal individuals extant before the fire suppression transformation; 2) Janzen–Connell effect driven by a soil pathogen operating on the *P. serotina* (Packer and Clay, 2000); and 3) Janzen–Connell effect driven by a beetle seed predator operating on *H. virginiana* (De Steven, 1982, 1983*b*). Constructing a simple "toy" model that takes these three forces in combination produces a spatial pattern that is qualitatively similar to the pattern we currently observe in nature. From there we project the model in the "future" to see how long this spatial structure persists, specifically we want to know whether distinct *P. serotina* and *A. rubrum* patches remain when the two become the dominant overstory species.

## 4.2 Methods

The forest is located in the E. S. George Reserve, Livingston County in southeast Michigan, which is operated by the department of Ecology and Evolutionary Biology of the University of Michigan. In a permanently marked 22-ha plot, called the Big Woods Plot, we have located, measured, and marked all individuals greater than 10cm in girth at breast height (GBH). An original 12ha plot was set up in 2003 and in 2008 this plot was re-censused and the other 10 hectares were added. So for more than half the plot we have five-year growth, mortality, and recruitment into the >10cm GBH size class. In all there are over 25,000 individuals in the plot. Further details on the site and census methodology can be found in Jedlicka and Vandermeer (2004).

The upper canopy (greater than 100cm GBH) of the forest is dominated (over

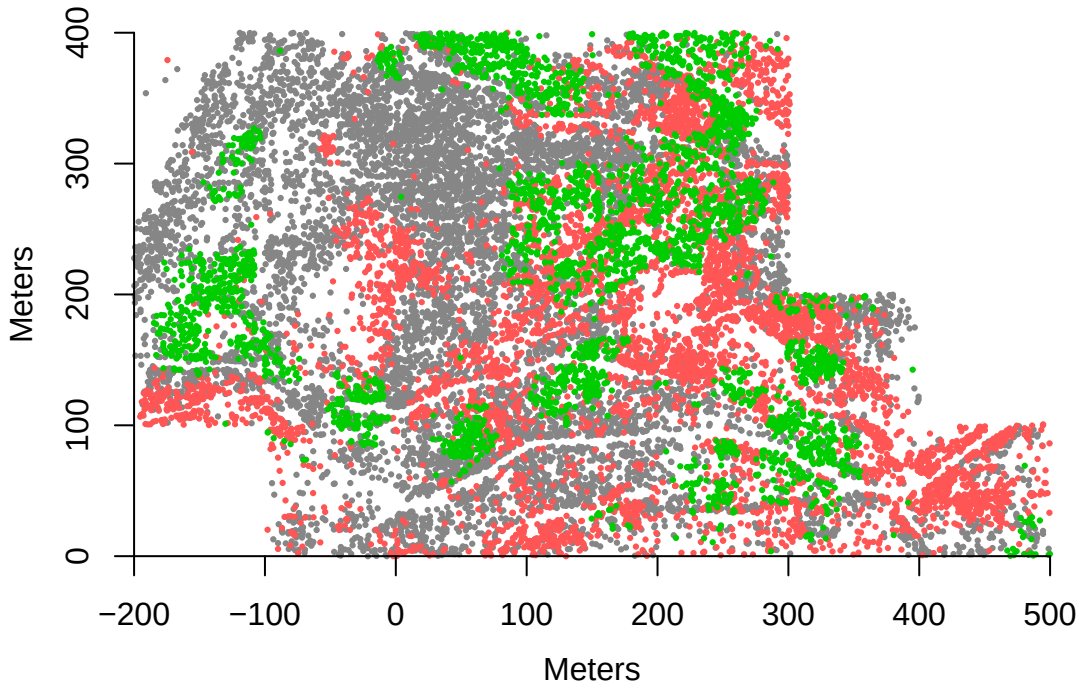


Figure 4.1: The mosaic spatial pattern of the Big Woods understory (less than 50cm GBH). *P. serotina* is gray, *A. rubrum* is red, and *H. virginiana* is green. The southern (bottom) of the plot borders a large swamp. The two empty areas right-center are ephemeral ponds, the plot abuts an old field on its upper-left border, and the long empty spaces are roads.

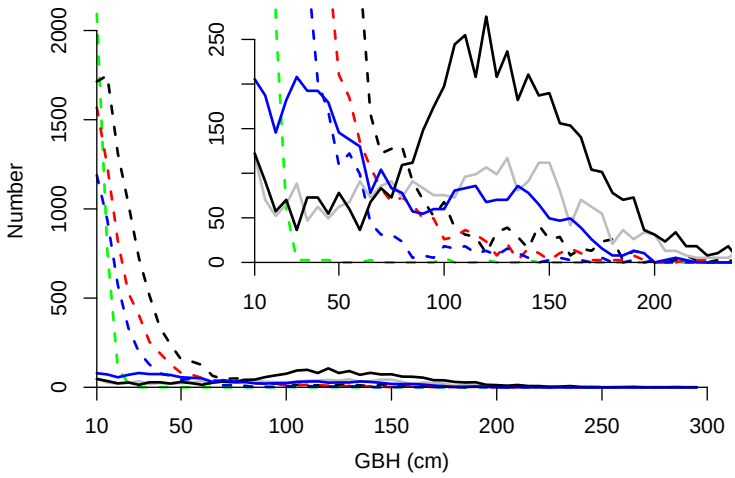


Figure 4.2: Frequency distribution of GBHs in the Big Woods Plot separated by species for the major species in the plot. Dashed green is *H. virginiana*, dashed red *A. rubrum*, dashed black *P. serotina*, solid blue *Carya* spp., solid gray *Q. alba*, solid black *Q. velutina*, and dashed blue all other species.

85%) by *Quercus alba*; "black oak" a hybrid swarm of *Q. velutina*, *Q. rubra*, and *Q. coccinea* (Voss, 1985), we shall just refer to these as *Q. velutina*; *Carya glabra*; *C. ovata*; and *C. cordiformis*. On the other hand these five species make up under 5% of the subcanopy (less than 50cm GBH), instead the subcanopy is dominated by (over 77%) *Hamamelis virginiana*, *Acer rubrum*, and *Prunus serotina*. A frequency distribution of GBHs separated by species gives a picture of the current state of the forest (Figure 4.2). The share of *Carya* and *Quercus* in both the upper canopy and the subcanopy decreased between 2003 and 2008, since their mortality is high—8% over the five-year period—and there is little recruitment. At the same time the fraction of trees greater than 100cm GBH—presumably canopy trees—that are *P. serotina* and *A. rubrum* increased, going from 13.8% in 2003 to 20.0% in 2008 and from 11.9% to 14.0% respectively.

As the current *Carya* and *Quercus* in the canopy die, they are increasingly be replaced by *Acer rubrum* and *Prunus serotina*. The *Carya*–*Quercus* dominance is thought to be a consequence of fires set by Native Americans, probably for hunting,

or perhaps escaped from agriculture. Subsequent to the fire suppression brought on by European colonists, fire-sensitive species have increased in number and their shading has prevented the recruitment of *Quercus* and *Carya*. Abrams (1992, 1998) developed this theory to explain *Quercus* declines and an increase in *A. rubrum* seen in many northeastern North American forests. Others have reported similar changes (Zhang et al., 2000; McDonald et al., 2003; Heitzman et al., 2007; Dickmann and Leefers, 2006). This process is broadly consistent with even only casual observations in the Big Woods forest.

If this is the case we would expect that the largest *A. rubrum* and *P. serotina* would be found in fire refugia. To test this on October 2nd, 2011 we took 620 soil moisture readings across the big woods plot. We fit a LOESS surface, with smoothing parameter 0.175, to these readings to give us an estimate of the soil moisture at all locations within the plot (Cleveland and Devlin, 1988). We then compared the average soil moisture at the locations of the largest 1% of *A. rubrum* and *P. serotina* to the soil moisture of 1000 random placements of that many "trees."

To study potential a possible Janzen–Connell effect in *H. virginiana* we tagged fruits on individuals within a range of clump sizes and followed their on-tree survival over their development from fruit set in May to dispersal in September in the summer of 2008. Cause of mortality was classified as chipmunk or Lepidopteran larva feeding or *Pseudanthonomus helvolus* parasitization. We also collected litter samples ($1m^2$ samples) in the fall of 2009 in the various clusters of *H. virginiana* and paired these with litter samples outside of those clusters. From these samples we extracted the weevils using mini-Winkler extractors. This part of the study is described fully in Section 3.2.

The system was modeled on a 100-by-100 lattice with periodic boundaries. Each cell (lattice point) can take on one of six states: empty (which could also be thought of as a *Quercus* yet to fall), *H. virginiana*, small *A. rubrum*, large *A. rubrum*, small

*P. serotina* or large *P. serotina*. The state of a cell depends on the state of that cell and its neighbors at the previous time step. Empty cells receive propagules from neighboring *H. virginiana*, large *A. rubrum*, and large *P. serotina*, and become a *H. virginiana*, small *A. rubrum*, or small *P. serotina* with probability proportional to the number of propagules received. The size of that neighborhood differs for the three species to represent the differing dispersal abilities. The Janzen–Connell effect is introduced into the model by the number of propagules created by a *H. virginiana* cell decreasing with the number of other *H. virginiana* in its neighborhood, and empty cells next to large *P. serotina* failing to become inhabited by small *P. serotina*.[1] These rules correspond to what is known specifically about the spatially specific natural enemy dynamics of those two species. *H. virginiana*, large *A. rubrum*, and large *P. serotina* cells become empty (adult mortality) with a given probability or stay the same at each time step. Small *A. rubrum*, and small *P. serotina* cells can become large, stay the same, or die (become empty) with probabilities depending on the number of neighboring large cells of either species. The model is initiated from a lattice with 98% of the cells empty and the remaining 2% evenly divided between *H. virginiana*, large *A. rubrum*, and large *P. serotina*. The location of these trees corresponds to the location of the largest *H. virginiana*, *A. rubrum*, and *P. serotina* in the actual plot, as an approximation for the distribution of these trees at the time of European fire suppression. A complete description of the model and the R code to run it can be found in the Appendix: Model Description.

## 4.3 Results

The three dominant subcanopy species form a tight jigsaw-puzzle-like mosaic (Figure 4.1). The largest 1% of *P. serotina* and *A. rubrum* correlate with the wettest

[1] That is not to say that we think there are no negative density-dependent mechanisms acting on *A. rubrum*, but just that the ones acting on *H. virginiana* and *P. serotina* are most responsible for the spatial pattern observed

regions of the plot (Figure 4.3). The largest 1% of *P. serotina* individuals occur in locations with an average soil moisture of 74.3%. Only 0.06% of random placements of this many individuals occurred in locations with an average soil moisture of this value or higher. The largest 1% of *A. rubrum* occur in locations with an average soil moisture of 73.6%, and only 2.27% of random placements of this many individuals occurred in locations with this soil moisture or higher. This is consistent with our hypothesis that the largest, and thus oldest, of these trees occupy fire refugia, although there are alternative explanations.

Since these largest trees are also presumably the oldest seed source for these species in the area we expect that their conspecifics should be clustered around them. This can be seen in Figure 4.4. Indeed for *H. virginiana* (Figure 4.4a) the largest individuals form the 'backbone' of most clumps, and small stems are significantly clumped around larger stems at a range of spatial scales (Figure 4.5). For a more complete examination of this pattern see Chapter III.

The same pattern is seen, though not as tightly, with *A. rubrum* (Figure 4.4b). The small stems cluster around larger stems at an intermediate scale, though, strangely, not at a small scale (Figure 4.6). As we shall see below, this scale effect is probably due to a "release" effect provided by the action of a soil pathogen on the major competitor of the *A. rubrum*.

This pattern of smaller (younger) trees clusterd around the older, presumably seed sources, is definitely not seen with *P. serotina*: in fact it shows the opposite trend. *P. serotina* individuals show striking evidence of a stand-level Janzen–Connell effect with small- to mid-size trees most dense in areas farther away from large trees (Figure 4.4c). This pattern is statistically significant, with fewer small- to mid-size trees between 0 and 25 meters from larger trees than predicted by a Poisson distribution of trees (Figure 4.7). This is consistent with what is expected from the operation of a soil pathogen, *Pythium* spp. (Oomycota), known to build up in the soil around larger

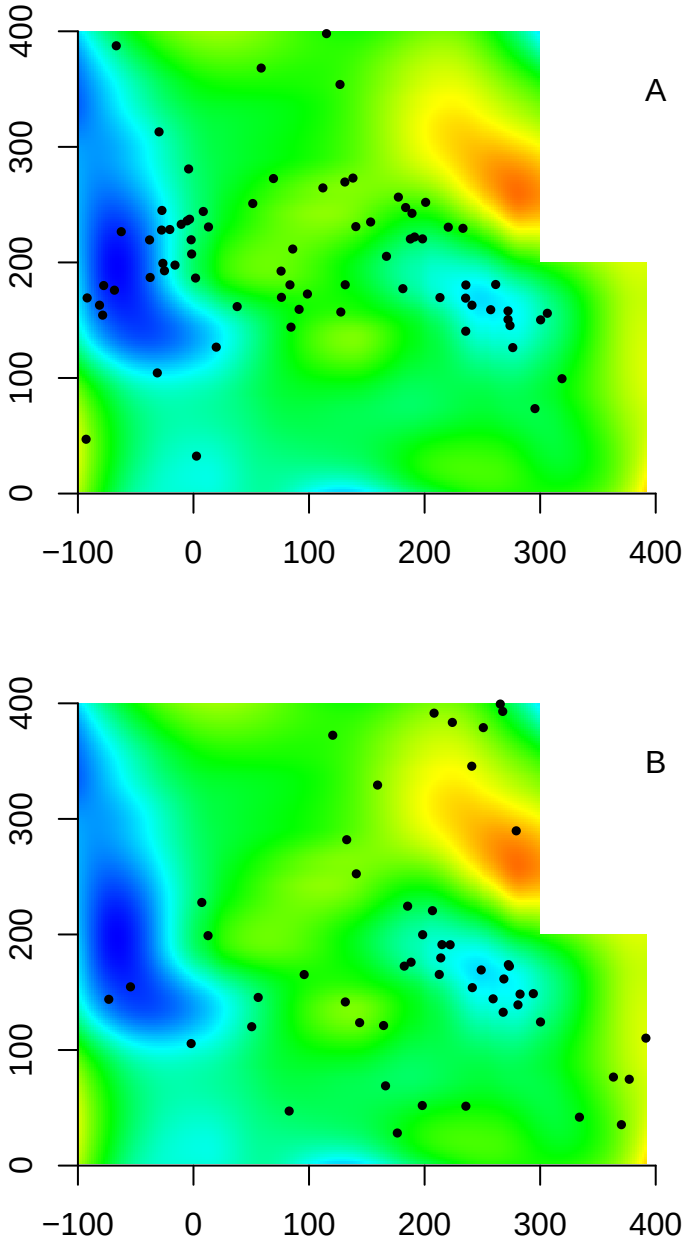


Figure 4.3: The locations of the largest 1% of *P. serotina* (A) and *A. rubrum* (B) plotted over the estimated soil moisture. The soil moisture is indicated by color with blue the wettest 90% soil moisture and red the driest 40% soil moisture. Both of these sets of trees occur in wetter regions than random. We interpret this to be evidence that they are growing in areas that used to be fire refugia.

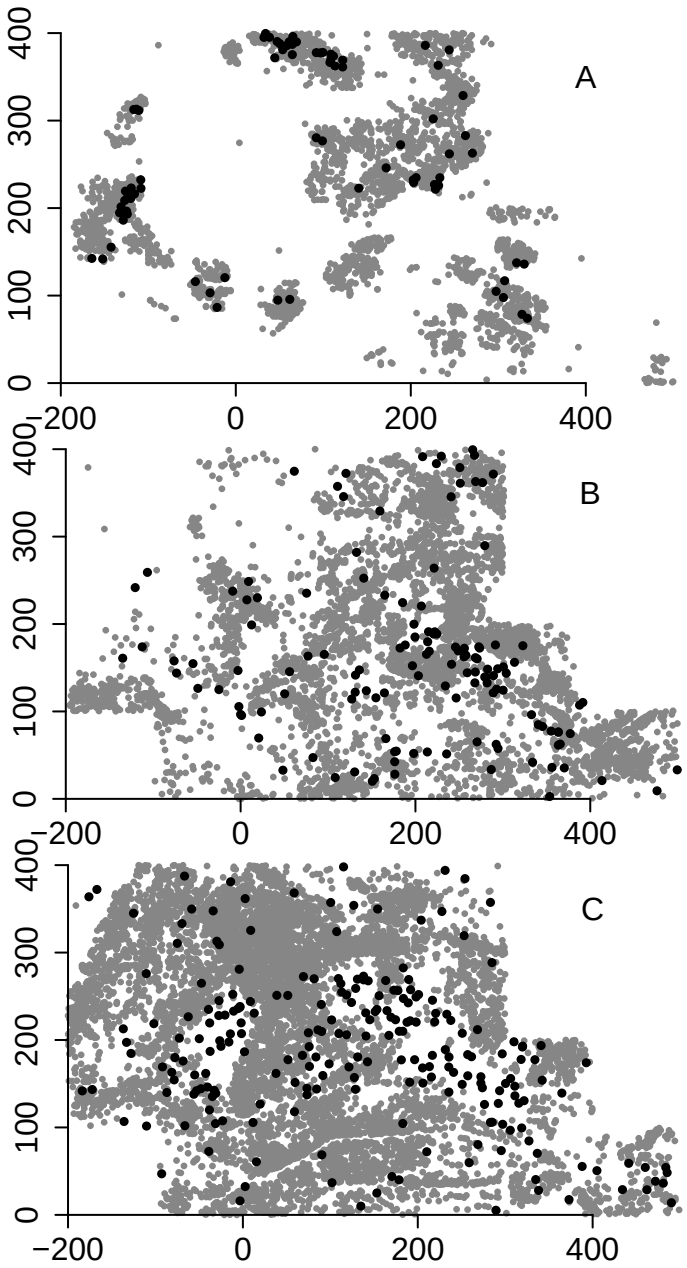


Figure 4.4: The distribution of large (black) and small (grey) individuals of the three major understory species, illustrating three distinct patterns. A) *H. virginiana* individuals with the largest (by GBH) 5% highlighted. Note the clear clusters of smaller trees surrounding the larger, presumably seed source, trees. B) *A. rubrum* individuals with the largest 5% highlighted, illustrating a more continuous spread of smaller individuals from the presumed seed sources. C) *P. serotina* individuals with the largest 5% highlighted, showing the striking pattern of smaller individuals effectively excluded from large areas where the larger, and presumably seed source, trees are located.

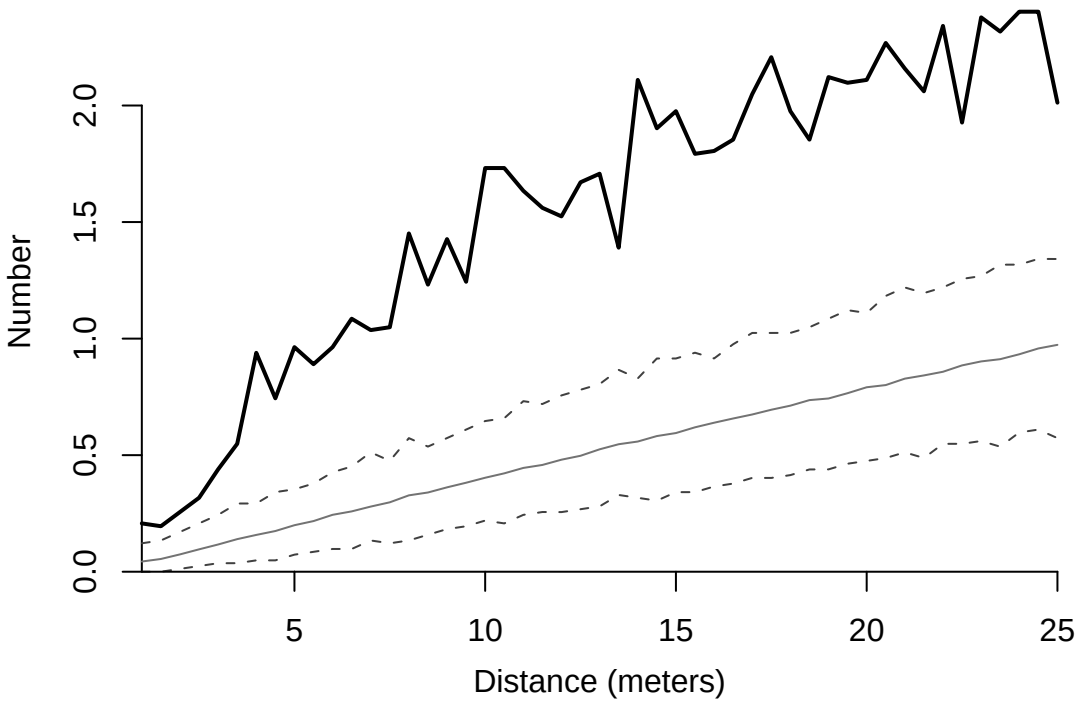


Figure 4.5: Average number of small (<15 cm GBH) *H. virginiana* found within 0.5-meter wide "donuts" a given distance around large (>20 cm GBH) *H. virginiana*. The black line is the observed value and the gray the Poisson expectation.

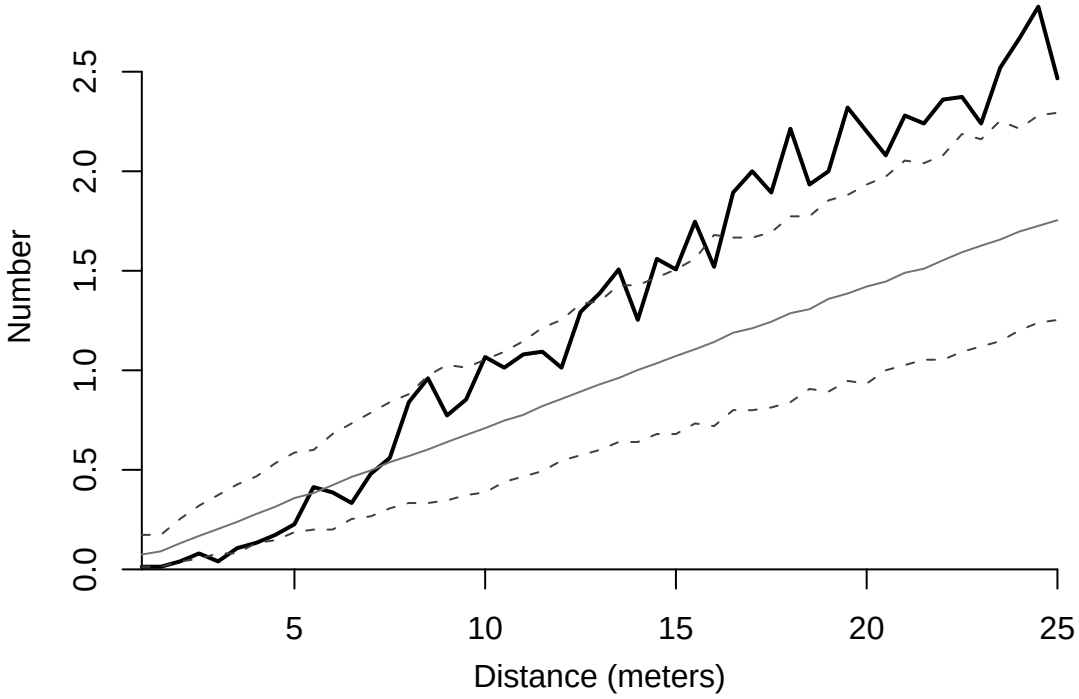


Figure 4.6: Average number of small (<50 cm GBH) *A. rubrum* found within 0.5-meter wide "donuts" a given distance around large (>100 cm GBH) *A. rubrum*. The black line is the observed value and the gray the Poisson expectation.

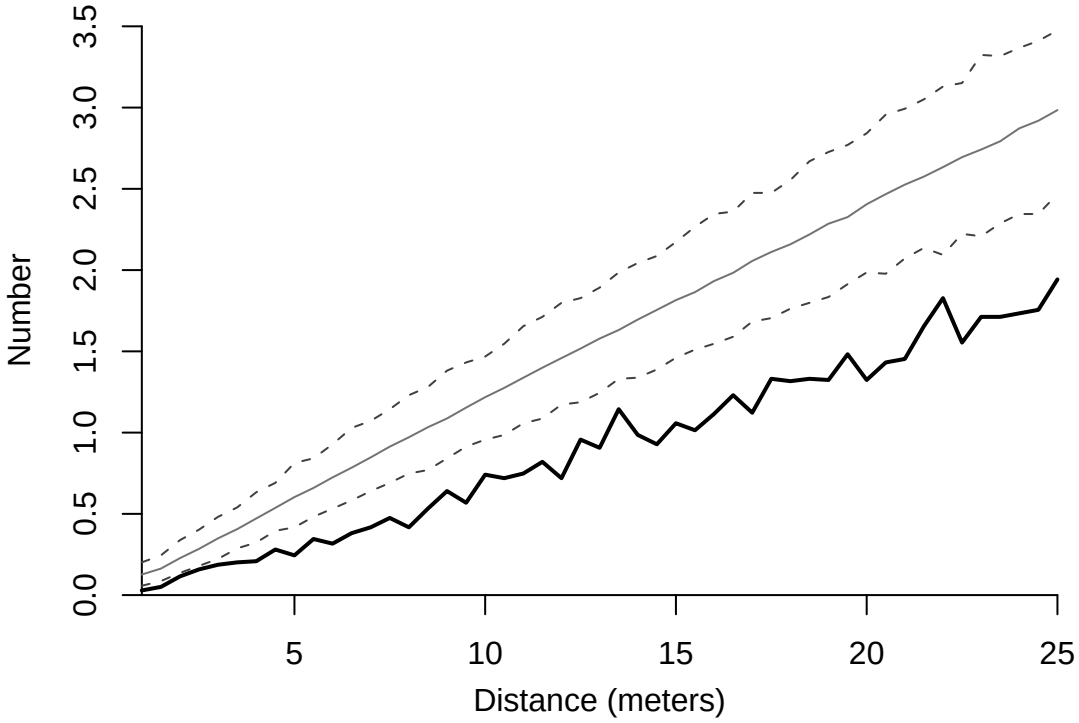


Figure 4.7: Average number of small (<50 cm GBH) *P. serotina* found within 0.5-meter wide "donuts" a given distance around large (>100 cm GBH) *P. serotina*. The black line is the observed value and the gray the Poisson expectation.

*P. serotina* individuals thus reducing recruitment, growth, and survival of conspecific seedlings (Packer and Clay, 2000, 2003; Reinhart et al., 2003, 2005).

*H. virginiana* also shows evidence of Janzen–Connell effect. Non-aborted fruits on trees in large patches had a lower survival rate than those in smaller patches or isolated individuals (Figure 3.5). Most of this seed mortally was due to *P. helvolus*, a *H. virginiana*-specific weevil seed parasite (De Steven, 1982, 1983*b*; Clark, 1987). Furthermore, the litter samples revealed a higher population density of beetles within clusters of *H. virginiana* (0.77 beetles per sample with $\pm$ 0.19 standard error) compared to zero found in paired sites outside clusters, suggesting that local build-up of the seed predator population is driving Janzen–Connell effect.

From these observations we propose a system of recruitment limitation coupled

with interspecific competition and the Janzen–Connell effect that leads to the observed pattern (Figure 4.1). With European fire suppression recruitment of *H. virginiana* and *A. rubrum* was limited to areas around seed trees that had been concentrated in fire refugia. As *H. virginiana* patches grew larger their fecundity decreased, due to Janzen–Connell effect operating through the beetle seed predator. *P. serotina*, on the other hand, has a larger dispersal potential from its bird dispersal syndrome which, when combined with Janzen–Connell effect resulting from the soil pathogen, causes young *P. serotina* trees to be concentrated in areas far from the larger *P. serotina*. *A. rubrum* directly reflects the dispersal from fire refugia, constrained, at least temporarily, from competition from the other two species, and is thus more concentrated in those areas with larger individual *P. serotina*, being able to avoid competition from seedlings of the latter because of the pattern induced by the Janzen–Connell effect.

These features motivate the simple discrete-time cellular automata model as described in the Appendix: Model Description. The model is not meant to be carefully fit and produce quantitative predictions, but rather to show that it is possible that these processes could give rise to the pattern seen. One run of the model, after ten iterations, is shown in Figure 4.8 (the parameters are shown in Table 4.1, it is run one). It produces patterns qualitatively similar to those observed (compare with Figure 4.1). *H. virginiana* and *A. rubrum* patches grow around the initial trees while *P. serotina* fill in the space farther away from large initial *P. serotina* and a tight spatial mosaic emerges quickly.

To get a sense for the variation in pattern produced we ran the model with other parameter sets (summarized in Table 4.1). After ten iterations most of these runs look like the pattern we observed (Figure 4.9). To see what this model says about the future of the forest we let it run into the "future." These are also shown in Figure 4.9.

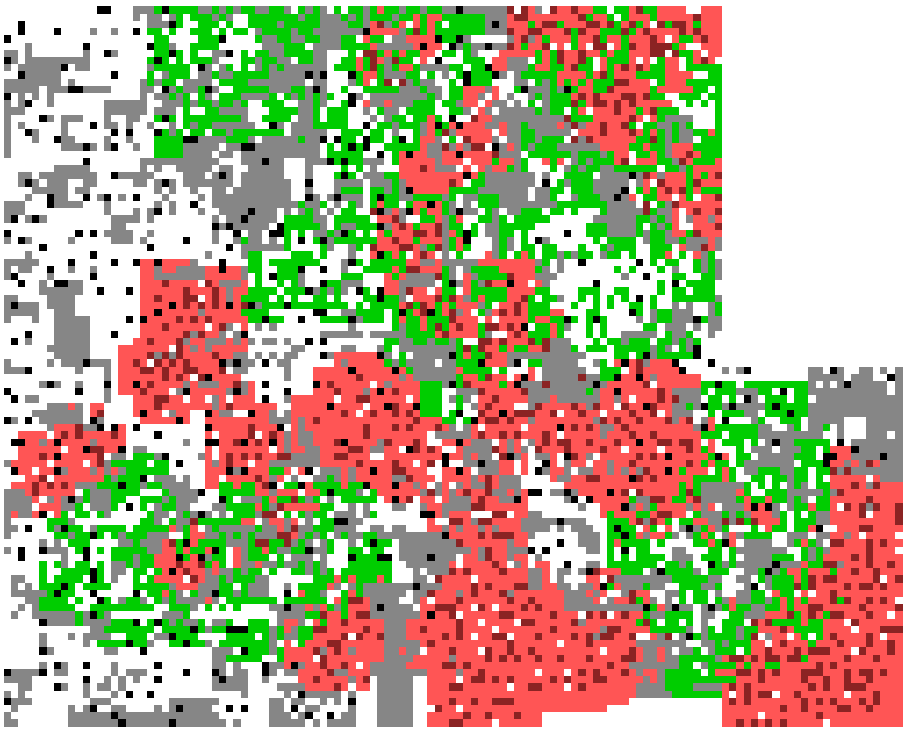

Figure 4.8: Example output from the cellular-automata model that simulated Big Woods understory-tree dynamics. Large *P. serotina* are black, small *P. serotina* gray, large *A. rubrum* dark red, small *A. rubrum* light red and *H. virginiana* green. Note the mosaic pattern, reflecting a similar pattern to that observed in nature (Figure 4.1).

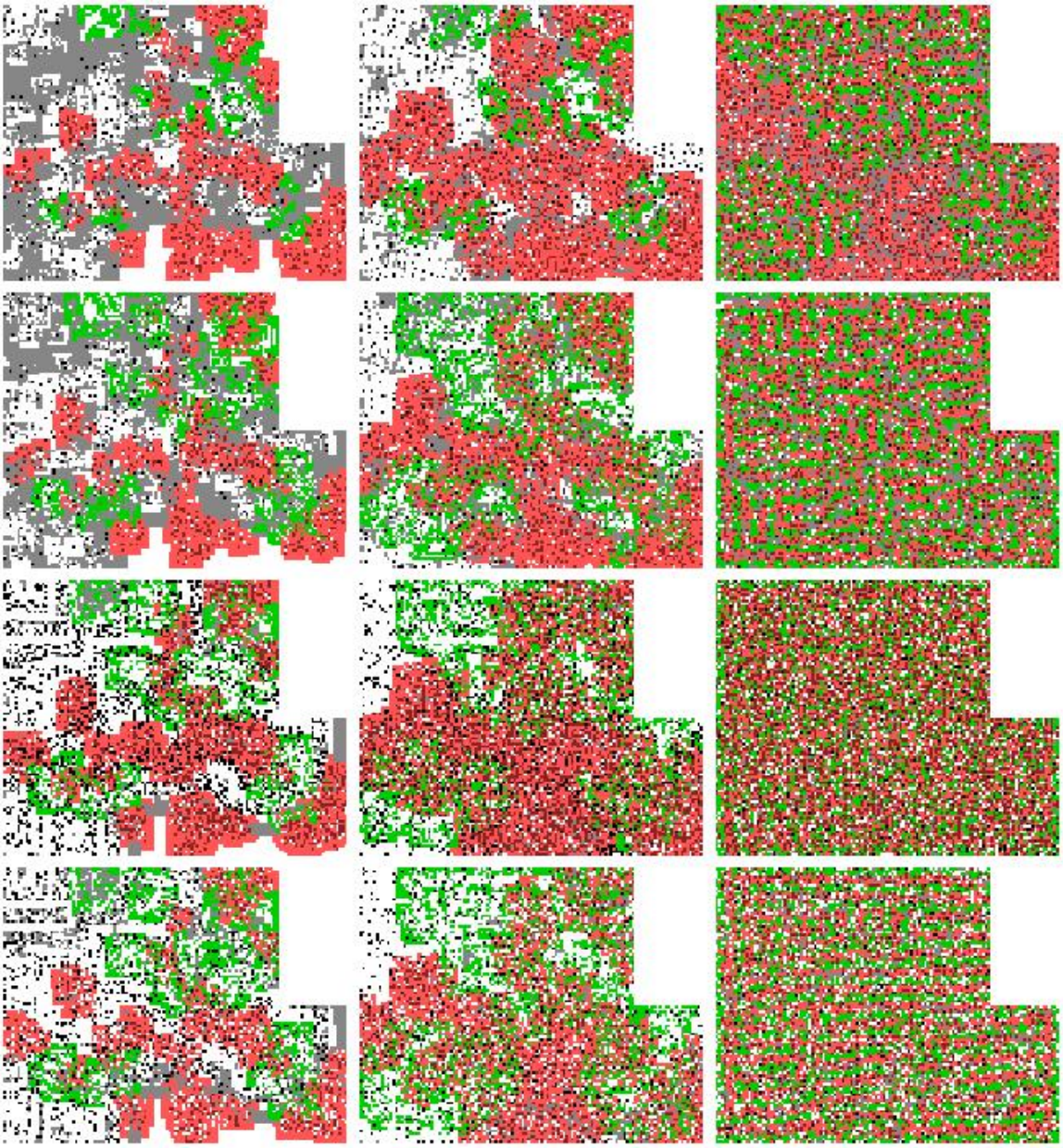

Figure 4.9: Results from the cellular-automata model that simulates the Big Woods understory-tree dynamics. Large *P. serotina* are black, small *P. serotina* gray, large *A. rubrum* dark red, small *A. rubrum* light red and *H. virginiana* green. The four rows are for parameter sets one through four parameter sets (Table 4.1), and the three columns are for five, ten and 50 iterations.

| Name | Run 1 | Run 2 | Run 3 | Run 4 |
|---|---|---|---|---|
| *P. serotina* large mortality | 0.1 | 0.1 | 0.1 | 0.15 |
| *A. rubrum* large mortality | 0.1 | 0.1 | 0.1 | 0.15 |
| *H. virginiana* mortality | 0.05 | 0.1 | 0.33 | 0.33 |
| *P. serotina* small-to-large intercept | 0.03 | 0.03 | 0.25 | 0.15 |
| *P. serotina* small-to-large slope | -0.025 | -0.025 | -0.05 | -0.05 |
| *A. rubrum* small-to-large intercept | 0.1 | 0.1 | 0.25 | 0.15 |
| *A. rubrum* small-to-large slope | -0.033 | -0.033 | -0.05 | -0.05 |
| *P. serotina* small mortality slope | 0.25 | 0.25 | 0.2 | 0.2 |
| *P. serotina* small mortality intercept | 0.001 | 0.001 | 0.05 | 0.01 |
| *A. rubrum* small mortality | 0.05 | 0.05 | 0.1 | 0.2 |
| *H. virginiana* Janzen–Connell parameter | 0.025 | 0.05 | 1 | 0.5 |

Table 4.1: Parameters for the Big Woods simulation model.

## 4.4 Discussion

Here we have argued that the evident spatial pattern extant in the subcanopy of a transitional forest in eastern Michigan can be understood by a combination of historical forces, dispersal limitation, and Janzen–Connell effect operating on two of the three species. Normal seed dispersal from remnant large trees establishes the initial pattern which is then followed by adjustment from the action of Janzen–Connell effect dynamics. The consequence is a jigsaw-like pattern that appears relatively stable, at least for the medium term. Our simple model which incorporates our understanding of the forest's history and these dynamics reproduces these patterns.

It is clear that the formerly dominant *Quercus* and *Carya* species are not replacing themselves as adults fall from the canopy. They are being replaced by *A. rubrum* and *P. serotina* as is happening in many places in eastern North America (Abrams, 1998, 1992; Zhang et al., 2000; Heitzman et al., 2007; McDonald et al., 2003; Dickmann and Leefers, 2006). This processes is playing out in a strongly spatially structured forest. Projecting our simple model forward suggests that as *A. rubrum* and *P. serotina* enter the canopy in large numbers their spatial structuring will begin to break down and the forest will become more well-mixed. Under some scenarios (parameter sets) other spatial patterns emerge and persist. For example with parameter sets one and

two tighter, more regular patches of *H. virginiana* emerges, these resemble Turing-instability patches often seen in patterned vegetation (van de Koppel et al., 2005; Rietkerk et al., 2002; Klausmeier, 1999). The model here is not to predict exactly how the forest structure will change, but to present a range of possibilities based on the major forces we think are currently structuring the forest.

## 4.5 Appendix: Model Description

Our Big Woods simulation model was a cellular automata where each cell could take one of six states: empty, large or small *P. serotina*, large or small *A. rubrum*, or *H. virginiana*. The model takes place on a 100-by-100 grid.

We calibrated the dispersal potential of each species by considering neighborhoods of varying sizes around the central cell. In particular, empty cells receive 1/120th of a propagule from any large *P. serotina* in the 11-by-11 square of cells surrounding it, 1/48th of a propagule from any large *A. rubrum* in the 7-by-7 square of cells surrounding it, and propagules from any *H. virginiana* in the 3-by-3 square of cells surrounding it. The number of propagules from each *H. virginiana* is $\frac{1/8}{n_1 p_1}$ where $n_1$ is the number of other *H. virginiana* in the 7-by-7 square of cells surrounding the focal *H. virginiana*. If there are any large *P. serotina* in the 3-by-3 square of cells surrounding it, it becomes a *H. virginiana* or small *A. rubrum* with probability proportional to the number of *H. virginiana* propagules and *A. rubrum* propagules it receives. Otherwise it becomes a *H. virginiana*, small *A. rubrum* or small *P. serotina* with probability proportional to the number of propagules of each it receives.

Small *P. serotina* become large with probability $(p_2+p_3)n_2$, where $n_2$ is the number of large trees (of both species) within the 3-by-3 square of cells surrounding it, and die with probability $(p_4 + p_5)n_3$, where $n3$ is the number of large *P. serotina* within the 3-by-3 square of cells surrounding it otherwise they remain small. Similarly for *A. rubrum* which become large with probability $(p_6 + p_7)n_2$, die with probability $p_8$,

and stay small otherwise. Large *P. serotina*, large *A. rubrum* and *H. virginiana* cells become empty with probability $p_9$, $p_10$ and $p_11$ , respectively, and otherwise stay the same. The R code to run the model follows.

```
# David Allen (dnallen@umich.edu) and John Vandermeer
# for the manuscript 'Dual Janzen--Connell
#effects create spatial pattern in a temperate successional forest'
# model to simulate interaction of Red Maple, Black Cherry and Witch Hazel

setwd('')
#starting from big tree locations
load('big_tree_loc.RData')

grid_len1 <- 125
grid_len2 <- 100

num_runs <- 7
par(bty='n')

################################################
################ demographic parameters ########
################################################

################  big to dead ##################
bc_m <- 0.1 # BC big mortality
rm_m <- 0.1 # RM big mortality
wh_m <- 0.1 # WH mortality

################  small to big ##################
bc_g_s <- -0.025
bc_g_i <-  0.03
rm_g_s <- -0.1/3
rm_g_i <-  0.1

################  small to dead ##################
bc_sm_s <-  0.25
bc_sm_i <-  0.001
rm_sm <-  0.05

################  J-C for WH   ###################
wh_param<- 0.075
```

```
#### Color map for display ##########
my_colors<-c('white','gray',rgb(0,0,0,1),rgb(1,0,0,0.5),'red','green3')

dis_ind<-1

for (run in 1:num_runs)
{
 N<-matrix(data=0,ncol=grid_len2,nrow=grid_len1)
 R<-matrix(data=runif(grid_len1*grid_len2),ncol=grid_len2,nrow=grid_len1)
 for (i in 1:grid_len1)
 {
  for (j in 1:grid_len2)
  {
   #empty cells
   if (M[i,j] == 0)
   {
    i8m<-ifelse(i-8>0.5,i-8,1)
    i7m<-ifelse(i-7>0.5,i-7,1)
    i6m<-ifelse(i-6>0.5,i-6,1)
    i5m<-ifelse(i-5>0.5,i-5,1)
    i4m<-ifelse(i-4>0.5,i-4,1)
    i3m<-ifelse(i-3>0.5,i-3,1)
    i2m<-ifelse(i-2>0.5,i-2,1)
    i1m<-ifelse(i-1>0.5,i-1,1)
    i8p<-ifelse(i+8<grid_len1+0.5,i+8,grid_len1)
    i7p<-ifelse(i+7<grid_len1+0.5,i+7,grid_len1)
    i6p<-ifelse(i+6<grid_len1+0.5,i+6,grid_len1)
    i5p<-ifelse(i+5<grid_len1+0.5,i+5,grid_len1)
    i4p<-ifelse(i+4<grid_len1+0.5,i+4,grid_len1)
    i3p<-ifelse(i+3<grid_len1+0.5,i+3,grid_len1)
    i2p<-ifelse(i+2<grid_len1+0.5,i+2,grid_len1)
    i1p<-ifelse(i+1<grid_len1+0.5,i+1,grid_len1)
    j8m<-ifelse(j-8>0.5,j-8,1)
    j7m<-ifelse(j-7>0.5,j-7,1)
    j6m<-ifelse(j-6>0.5,j-6,1)
    j5m<-ifelse(j-5>0.5,j-5,1)
    j4m<-ifelse(j-4>0.5,j-4,1)
    j3m<-ifelse(j-3>0.5,j-3,1)
    j2m<-ifelse(j-2>0.5,j-2,1)
    j1m<-ifelse(j-1>0.5,j-1,1)
    j8p<-ifelse(j+8<grid_len2+0.5,j+8,grid_len2)
    j7p<-ifelse(j+7<grid_len2+0.5,j+7,grid_len2)
    j6p<-ifelse(j+6<grid_len2+0.5,j+6,grid_len2)
    j5p<-ifelse(j+5<grid_len2+0.5,j+5,grid_len2)
    j4p<-ifelse(j+4<grid_len2+0.5,j+4,grid_len2)
```

```
 j3p<-ifelse(j+3<grid_len2+0.5,j+3,grid_len2)
 j2p<-ifelse(j+2<grid_len2+0.5,j+2,grid_len2)
 j1p<-ifelse(j+1<grid_len2+0.5,j+1,grid_len2)

 neigh_8<-c(M[i8m:i8p,j8p:j1p],M[i8m:i8p,j8m:j1m],M[i8p:i1p,j],M[i8m:i1m,j])
 neigh_7<-c(M[i7m:i7p,j7p:j1p],M[i7m:i7p,j7m:j1m],M[i7p:i1p,j],M[i7m:i1m,j])
 neigh_6<-c(M[i6m:i6p,j6p:j1p],M[i6m:i6p,j6m:j1m],M[i6p:i1p,j],M[i6m:i1m,j])
 neigh_5<-c(M[i5m:i5p,j5p:j1p],M[i5m:i5p,j5m:j1m],M[i5p:i1p,j],M[i5m:i1m,j])
 neigh_4<-c(M[i5m:i4p,j4p:j1p],M[i4m:i4p,j4m:j1m],M[i4p:i1p,j],M[i4m:i1m,j])
 neigh_3<-c(M[i3m:i3p,j3p:j1p],M[i3m:i3p,j3m:j1m],M[i3p:i1p,j],M[i3m:i1m,j])
 neigh_2<-c(M[i2m:i2p,j2p:j1p],M[i2m:i2p,j2m:j1m],M[i2p:i1p,j],M[i2m:i1m,j])
 neigh_1<-c(M[i1m:i1p,j1p],M[i1m:i1p,j1m],M[i1p,j],M[i1m,j])

 wh_weev<-length(neigh_4[neigh_4==5])
 rm_seed<-length(neigh_3[neigh_3==4])/100
 wh_seed<-ifelse(wh_weev>0.5,length(neigh_2[neigh_2==5])/(wh_weev^wh_param),0)
 wh_seed<-ifelse(wh_weev>20,0,wh_seed)
 bc_seed<-length(neigh_5[neigh_8==2])/40
 bc_para<-length(neigh_3[neigh_3==2])


 seeds<-wh_seed + rm_seed + ifelse(bc_para>0.5,0,bc_seed)
 N[i,j]<-ifelse(seeds==0,0,
         ifelse(R[i,j]*seeds<wh_seed,5,
         ifelse(R[i,j]*seeds<wh_seed+rm_seed,3,1)))
}

#small black cherry
if (M[i,j] == 1)
{

 i1m<-ifelse(i-1>0.5,i-1,1)
 i1p<-ifelse(i+1<grid_len1+0.5,i+1,grid_len1)
 j1m<-ifelse(j-1>0.5,j-1,1)
 j1p<-ifelse(j+1<grid_len2+0.5,j+1,grid_len2)

 i2m<-ifelse(i-2>0.5,i-2,1)
 i2p<-ifelse(i+2<grid_len1+0.5,i+2,grid_len1)
 j2m<-ifelse(j-2>0.5,j-2,1)
 j2p<-ifelse(j+2<grid_len2+0.5,j+2,grid_len2)

 neigh_1<-c(M[i1m:i1p,j1p],M[i1m:i1p,j1m],M[i1p,j],M[i1m,j])
 neigh_2<-c(M[i2m:i2p,j2p:j1p],M[i2m:i2p,j2m:j1m],M[i2p:i1p,j],M[i2m:i1m,j])

 big_neigh<-length(neigh_1[neigh_1==2 | neigh_1==4])
```

```
 big_bc_neigh<-length(neigh_2[neigh_2==2])

 small_to_big <- bc_g_i + bc_g_s*big_neigh
 small_to_dead <- bc_sm_i + bc_sm_s * big_bc_neigh


 N[i,j]<-ifelse(R[i,j]< small_to_big,2,ifelse(R[i,j] > 1- small_to_dead, 0,1))
}

#big black cherry
if (M[i,j] == 2)
{
 N[i,j]<-ifelse(R[i,j]<bc_m,0,2)
}

#small red maple
if (M[i,j] == 3)
{
 i1m<-ifelse(i-1>0.5,i-1,1)
 i1p<-ifelse(i+1<grid_len1+0.5,i+1,grid_len1)
 j1m<-ifelse(j-1>0.5,j-1,1)
 j1p<-ifelse(j+1<grid_len2+0.5,j+1,grid_len2)

 neigh_1<-c(M[i1m:i1p,j1p],M[i1m:i1p,j1m],M[i1p,j],M[i1m,j])
 big_neigh<-length(neigh_1[neigh_1==2 | neigh_1==4])

 small_to_big <- rm_g_i + rm_g_s*big_neigh
 small_to_dead <- rm_sm

 N[i,j]<-ifelse(R[i,j]< small_to_big,4,ifelse(R[i,j] > 1- small_to_dead, 0,3))

}

#big red maple
if (M[i,j] == 4)
{
 N[i,j]<-ifelse(R[i,j]<rm_m,0,4)
}

#witch ahzel
if (M[i,j] == 5)
{
 N[i,j]<-ifelse(R[i,j]<wh_m,0,5)
}
```

```
  } #j
 } #i
 M<-N
 print(run)
 if (run == num_runs)
 {
  image(M,col=my_colors,asp=1,xaxt='n',yaxt='n')
 }
} #runs
dev.off()
```

# CHAPTER V

# Deviation from a power law represents a signal of regime change in Michigan deciduous forest

## 5.1 Introduction

Confronting uncertainty in the condition of environmental variables, a great deal of attention has recently focused on the way in which ecosystems are likely to undergo regime changes, large rapid shifts that can occur in ecosystems and that are often attributed to alternative stable states (Scheffer and Carpenter, 2003). The search for ways to identify when an ecosystem is on the precipice of a regime change has thus become a major priority for ecological research (Scheffer and Carpenter, 2003; Kéfi et al., 2007; Rietkerk et al., 2004*a*; Solé et al., 1999). The challenge is to link known ecosystem principles with necessary changes, frequently done through complicated analytical modeling, as, for example, in the case of water use of xerophyllic plants (Kéfi et al., 2007). Empirical support for detection methods is frequently scant since measurements before, during and after the regime change are rarely available.

Here we report on the application of recent theoretical understanding of forest structure to the search for indications of regime change. From a theoretical point of view we use a popular form of metabolic theory (West et al., 2009) to predict the distribution of trunks in a forest and limbs on a tree. This theory has done a good

job explaining patterns observed in long-term forest dynamics plots (Enquist et al., 2009). We compare the predictions of this theory to the patterns observed in a forest undergoing a major transition in species composition. We find major deviations between the predictions of this theory and observed patterns in this transitioning forest. We suggest this technique, testing simple predictions of metabolic theory, as a tool to assess whether other forests are undergoing a regime shift.

## 5.2 Methods

The forest in question is located on the E.S. George Reserve near Ann Arbor, Michigan, property of the University of Michigan. It is a transitional forest, with an upper canopy dominated by *Quercus* spp. and *Carya* spp., and an understory dominated by *Prunus serotina* and *Acer rubrum*. The transition obviously underway is similar to many forests in Eastern North America, in which the so-called "Red Maple Paradox" (Abrams, 1998, 1992). The regime change from an *Quercus–Carya* forest to a *A. rubrum–P. serotina* forest is evident with not much more than a casual walk through this forest—most of the very big trees are *Quercus* or *Carya* and the smaller pole-size trees are usually *A. rubrum* or *P. serotina*. See Section 4.2 for a more complete discussion of this transition. A 22ha plot was established on this site and all trees greater than 10cm GBH were identified, measured and georeferenced—over 25,000 stems (Jedlicka and Vandermeer, 2004). The number of individuals from five species in each of 25 size classes is given in Table 5.1. Given its transitional state, this forest offers an opportunity to test methods of detecting when a system is on the border of regime change.

Following the metabolic theory (West et al., 2009) we assume that the "normal" condition of an intact forest is that sizes of both branches on individual trees and trunks in the forest follow a power-law distribution of the same scaling exponent. This theory also predicts that the average nearest neighbor distance between two

| GBH (cm) | *P. serotina* | *A. rubrum* | *Q. velutina* | *Q. alba* | *C. ovata* | *C. glabra* |
|---|---|---|---|---|---|---|
| 10 to 19 | 2751 | 2236 | 49 | 54 | 17 | 92 |
| 20 to 29 | 1825 | 1093 | 27 | 36 | 35 | 71 |
| 30 to 39 | 1032 | 541 | 18 | 44 | 21 | 94 |
| 40 to 49 | 479 | 278 | 19 | 34 | 22 | 90 |
| 50 to 59 | 263 | 133 | 25 | 46 | 14 | 73 |
| 60 to 69 | 171 | 85 | 19 | 46 | 9 | 53 |
| 70 to 79 | 85 | 55 | 34 | 61 | 6 | 43 |
| 80 to 89 | 78 | 48 | 60 | 51 | 3 | 22 |
| 90 to 99 | 44 | 36 | 92 | 49 | 3 | 22 |
| 100 to 109 | 35 | 18 | 119 | 47 | 3 | 28 |
| 110 to 119 | 20 | 25 | 134 | 53 | 7 | 32 |
| 120 to 129 | 11 | 12 | 157 | 66 | 2 | 31 |
| 130 to 139 | 23 | 9 | 132 | 54 | 4 | 34 |
| 140 to 149 | 21 | 8 | 122 | 58 | 6 | 32 |
| 150 to 159 | 18 | 7 | 115 | 50 | 2 | 25 |
| 160 to 169 | 6 | 10 | 90 | 33 | 0 | 21 |
| 170 to 179 | 15 | 2 | 65 | 37 | 0 | 12 |
| 180 to 189 | 11 | 2 | 54 | 21 | 0 | 4 |
| 190 to 199 | 7 | 2 | 32 | 21 | 0 | 5 |
| 200 to 209 | 1 | 1 | 16 | 16 | 0 | 1 |
| 210 to 219 | 4 | 2 | 18 | 7 | 0 | 1 |
| 220 to 229 | 1 | 2 | 7 | 3 | 0 | 0 |
| 230 to 239 | 2 | 3 | 9 | 4 | 0 | 0 |
| 240 to 249 | 1 | 3 | 1 | 2 | 0 | 0 |
| 250 to 259 | 0 | 0 | 0 | 0 | 0 | 0 |
| 260+ | 0 | 0 | 3 | 0 | 0 | 0 |

Table 5.1: Basal stem size classes of five common species in the Big Woods plot.

stems in a given size class scales linearly with the DBH of trees within that size class on a log-log plot. To assess the first prediction we located individuals either of smaller trees or naturally wind-thrown larger trees and measured the diameters of every branch larger than 5cm in cirumference. From our Big Woods data set we found the DBH of all trunks, and calculated the nearest neighbor distance by size class.

Fitting power laws by least squares linear fit of log-log frequency distributions is problematic (White et al., 2008; Clauset et al., 2009). Thus we use the maximum-likelihood method of Clauset et al. (2009). We also use Clauset et al.'s (2009) good-of-fit test. The data set is compared to a power-law model using a Kolmogorov–Smirnov statistic. One thousand power-law distributed synthetic data sets with the same $\alpha$ and same number of observations, $n$, are created. Each of the synthetic data sets is compared to its own power-law model using the Kolmogorov–Smirnov statistic. The fraction of these synthetic data sets with a larger Kolmogorov–Smirnov statistic than the original data is the $p$-value. That is $p$ is the fraction of the time that the observed data looks more power-law distributed than synthetic data actually drawn from a power-law distribution. Clauset et al. (2009) rule out the power-law distribution if $p \leq 0.1$.

## 5.3 Results

Fitting a power-law distribution to the branch circumferences gives a scaling exponent of 2.67 (Figure 5.1). This fit is better, has a lower Kolmogorov–Smirnov statistic, than 25.1% of synthetic data sets drawn from the same power-law distribution. Thus there is relatively good support that these data are power-law distributed, as is predicted by the metabolic theory of West et al. (2009).

Fitting a power-law distribution to the GBHs of all the trees in the Big Woods gives a scaling exponent of 2.10 (Figure 5.2). But this is a poor fit, all of the synthetic

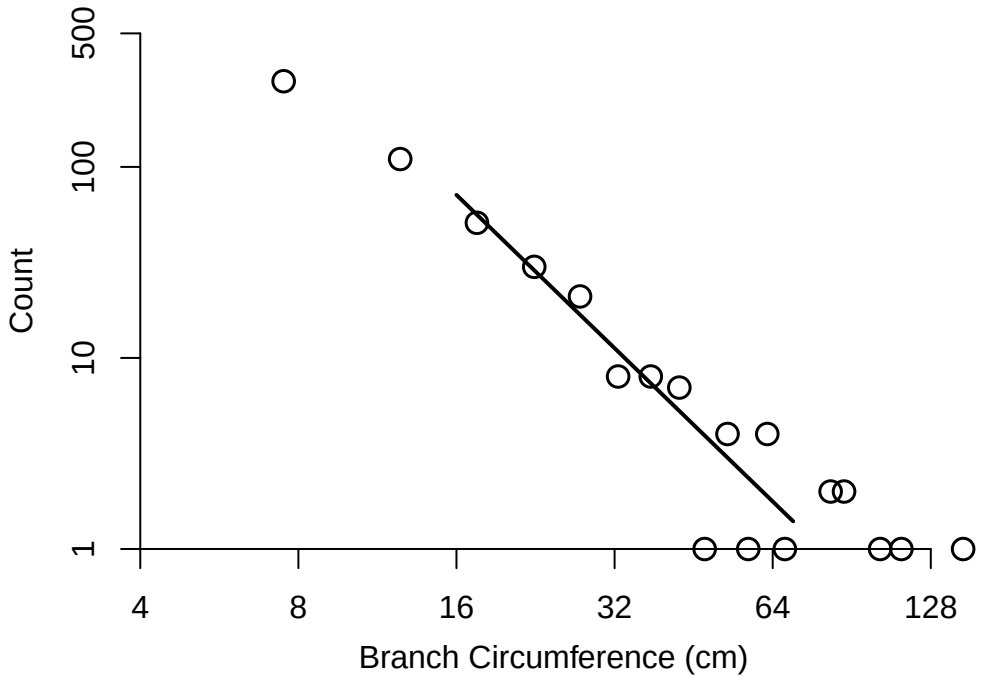


Figure 5.1: Frequency distribution of branch circumferences of wind-thrown trees in the Big Woods Plot on a log-log plot. The power law was fit with the maximum-likelihood methods of Clauset et al. (2009), not by with a least squares linear fit. The scaling exponent is 2.67, and Clauset et al.'s (2009) bootstrapping goodness-of-fit test supports—or at least does not reject—the power-law distribution.

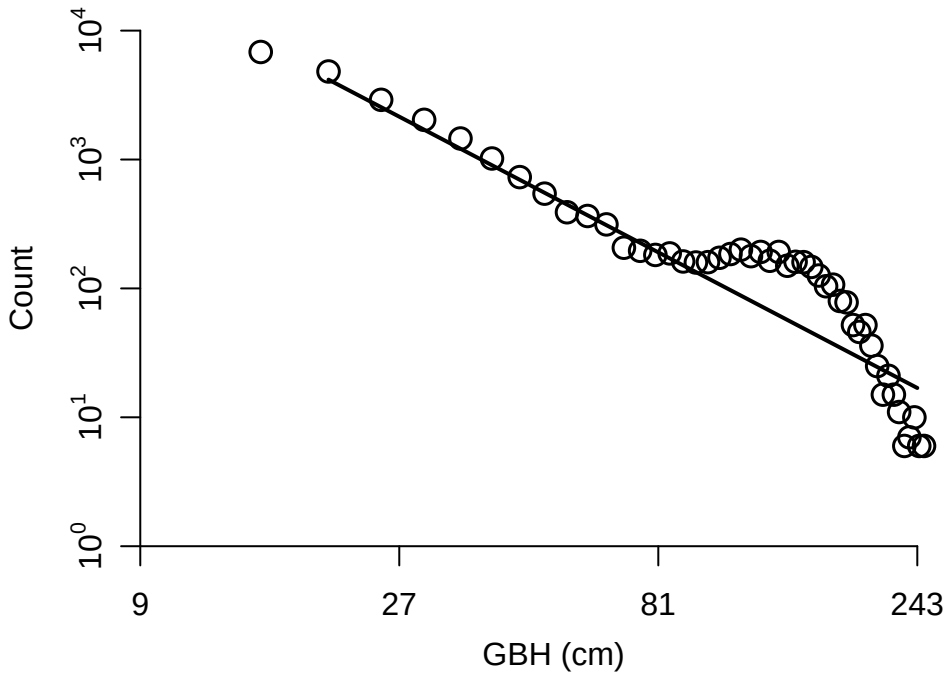


Figure 5.2: Frequency distribution of GBH of trees in the Big Woods Plot on a log-log plot. The maximum-likelihood power-law fit has a scaling exponent of 2.10, but Clauset et al.'s (2009) bootstrapping goodness-of-fit test rejects the power-law distribution.

data sets drawn from such a power-law distribution have a lower Kolmogorov–Smirnov statistic ($p = 0.000$). Thus we can safely reject a power-law distribution, a deviation from the predicts of West et al. (2009). From Figure 5.2 it is quite clear that this deviation comes from the bulge in number of trees with a GBH between 81 and 200cm; there are "too many" medium-to-large trees.

We know that the forest is undergoing a drastic change in species composition as the *Quercus* and *Carya* in the canopy die out and are replaced by other species. Also the size-distribution of these trees, especially the *Q. velutina*, in Table 5.1 shows a similar bugle in the same size range. Thus we repeated the power-law analysis of GBHs but with the *Quercus* and *Carya* removed. Now we get a scaling exponent of 2.51, and support ($p = 0.141$) that these GBHs are power-law distributed (Figure

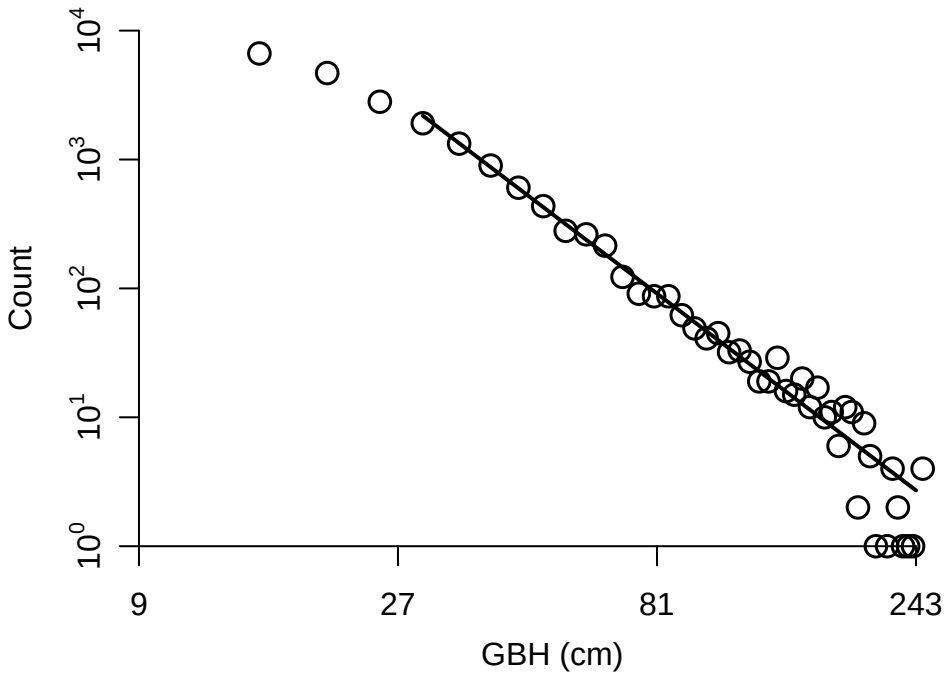


hh

Figure 5.3: Frequency distribution of GBH of trees in the Big Woods Plot with *Quercus* and *Carya* removed on a log-log plot. he maximum-likelihood power-law fit has a scaling exponent of 2.51. The power-law distribution is supported by Clauset et al.'s (2009) goodness-of-fit test.

5.3). Additionally this scaling exponent is quite close to the scaling exponent fit for the branches, as predicted by West et al.'s (2009) metabolic theory.

This forest deviates from other predictions of metabolic theory. Enquist et al. (2009) predict that the average distance between individuals within the same size class should scale linearly, on a log-log plot, with that size class's trunk size. They find close adherence to this prediction in Barro Colorado Island and San Emilio forest plots. Here we find middle-to-large sized trees closer together than expected by this prediction (Figure 5.4). Again if we remove the *Quercus* and *Carya* individuals the data fit the prediction.

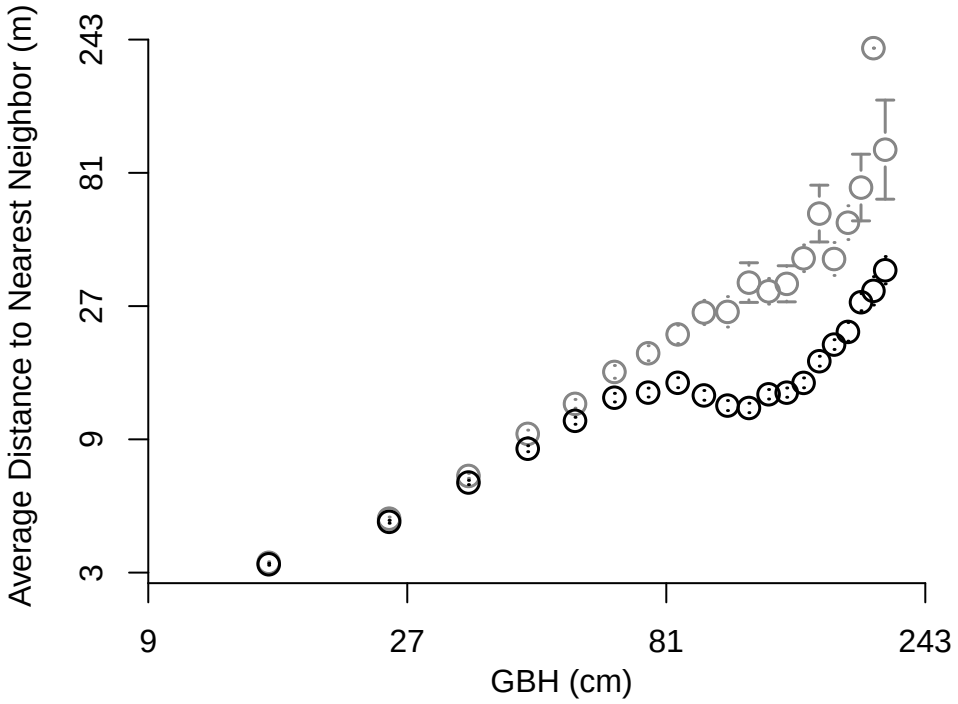


Figure 5.4: Average nearest neighbor distance between trees in the trunk-diameter size class. Each size class is 10 cm large. Standard error bars are indicated and when they are too small just with dashes. Black is for all trees and gray with the oaks and hickories removed. The metabolic theory of Enquist et al. (2009) predicts as linear relationship, as seen in the *Quercus*- and *Carya*-removed data. With those trees included the medium-to-large trees are closer together than predicted by the theory.

## 5.4 Dicussion

The Big Woods forest shows clear and systematic deviations for the predictions of West et al.'s (2009) metabolic theory and from the patterns observed in other forests (Enquist et al., 2009). At some level this is not surprising. That theory was developed for equilibrium communities, which this forest definitely is not. We know that the forest is undergoing a drastic change in species composition as the canopy *Quercus* and *Carya* are replaced by *P. serotina* and *A. rubrum* (see Section 4.2). This dynamic has been observed in other forests (Abrams, 1998; Zhang et al., 2000; Heitzman et al., 2007; McDonald et al., 2003). But these deviations offer an important insight into the structure of these changing forests. This forest is effectively a "normal" forest with extra medium- and large-sized *Quercus* and *Carya* packed into it. When these trees are removed we recover the patterns predicted by West et al. (2009). In fact although West et al.'s (2009) theory predicts a scaling exponent of about two, Enquist et al. (2009) found that in other mid-successional forests the exponent was much higher, as high as three. So our value of approximately 2.5 when me remove the *Quercus* and *Carya* is in line with other mid-successional forests.

Further this result shows that more generally deviation for the predictions of metabolic theory may provide a signal for regime change. Finding such signals is of great important (Scheffer and Carpenter, 2003; Kéfi et al., 2007). Here of course we have a good understanding of how this change will happen (see Chapter IV), but in other systems where the ecology is not as well understood *a priori* comparing against the predictions of a simple metabolic theory may offer a relatively easy test.

# CHAPTER VI

# When are habitat patches really islands?

## 6.1 Introduction

It is often the case that shabitats occur in a patchwork, vaguely suggestive of "islands" of suitable habitat in a "sea" of unsuitable habitat, and bringing to mind modern theoretical formulations, such as island biogeography. But is this framework legitimate? That is, do we have reason to believe that the habitat patchwork so common in terrestrial systems do indeed accord with what has come to be understood about "real" islands. The equilibrium theory of Island Biogeography (MacArthur and Wilson, 1967) makes predictions about the number of species inhabiting an island based on that island's size and distance from the mainland. It has been successful at explaining patterns of biodiversity on oceanic islands (Simberloff and Abele, 1976), some habitat island situations (Brown and Kodric-Brown, 1977), and most recently has provided a framework to think about biodiversity in fragmented landscapes (Simberloff and Abele, 1976). Here we suggest another application—that the predicted patterns of the theory could be used to infer whether the extinction/recolonization process is operative in a given system. This would allow one to determine whether, for a given set of species in a given landscape, a system of putative islands is really one of biological islands. A similar conceptual framework was put forth by Bond et al. (1988), but here we combine it with a modern resampling based statistical ap-

proach. We use this application to determine whether a particular system of island hummocks in a hardwood swamp in southern Michigan function as biological islands with regards to the trees growing on them.

The equilibrium theory of island biogeography assumes that on a given island extinctions are inevitable and take place at a rate inversely proportional to the size of that island. These extinctions are countered by recolonization of the island from the mainland, which happens at a rate inversely proportional to the distance from the mainland. The best way to test whether putative islands are biological ones would be to directly measure these extinction and colonization rates, but for long-lived organisms these processes take place over a time scale too large to easily measure. The theory of island biogeography provides predictions based on these assumptions of extinction/colonization species turnover that allow us to infer this turnover without directly measuring it. These predictions are: (1) larger islands have more species and (2) islands closer to the mainland have more species. If we take an "island" to be nothing more than a sample of a particular size embedded in the mainland, recolonizations of the "island" will happen at the greatest possible rate. This gives rise to a third prediction (3) islands should have fewer species than areas of equal size sampled on the mainland.

Here we test these three predictions in a system of eight terrestrial hummocks located in a swamp that abuts a *Quercus–Carya* forest. The tree flora on each island is evidently a subset of the tree flora of the nearby *Quercus–Carya* forest. If the above predictions are met for the pattern of tree diversity on the islands we can infer the extinction/recolonization turnover and thus the island nature of the hummocks. On the other hand if the predictions are not met, these hummocks are just extensions or samples of the nearby forest and the application of island thinking is illegitimate. We are additionally interested to see how these patterns differ if we look at trees of different successional stages within the forest.

## 6.2 Methods

The study site is part of the E.S. George Reserve, owned and operated by the University of Michigan consisting of a mosaic of forests, old fields and aquatic habitats. The terrestrial habitats have been strongly influenced by human activities, the old fields a consequence of row crops and pasture in the earlier parts of the twentieth century and the *Quercus–Carya* woodlots a likely consequence of fires resulting from Native American agriculture and hunting prior to European colonization.

The canopy of the forest is dominated by *Quercus alba* and "black" oak, the later being a hybrid swarm of *Q. velutina*, *Q. rubra*, and occasional *Q. coccinea* (Voss, 1985), as well as *Carya glabra*, *C. ovata*, and *C. cordiformis*. The *Quercus–Carya* dominance has been interpreted as a consequence of Native American hunting and agriculture and the fires escaped therefrom. Subsequent to fire exclusion with European colonization, the subcanopy and understory have been taken over by *Acer rubrum*, *Prunus serotina*, and *Hamamelis virginiana* , plus 15 other less common species, with very few *Quercus* in the subcanopy. This shift in species composition of some northeastern North American forests since European colonization—marked by a decrease in the number of *Quercus* and increase in the number of *Acer rubrum*—is well described (Abrams, 1998; Zhang et al., 2000; Heitzman et al., 2007; McDonald et al., 2003; Dickmann and Leefers, 2006). In an 12ha permanent plot on the "mainland" all trees greater 10cm GBH have been marked, measured, and mapped. This permanent plot will be referred to as the "mainland." Further details on the site and census methodology can be found in Jedlicka and Vandermeer (2004).

The hummocks are located in an extensive and diverse swampland, known locally as Big Swamp (Figure 6.1). The forest on each of these hummocks is similar to the mainland forest, with the tree flora on each a subset of the Big Wood tree flora. On each hummock two to four (depending on its length) 5m belt transects were conducted across the short dimension of the island and all trees with GBH greater

than 10cm were recorded. We ignored any individuals that grew right along the swamp-island border, as these were mostly swamp trees not colonists from the Big Woods. The transects were spaced evenly along the long axis of the island. Afterwards an observational sweep of the island was conducted to record any species that were missed in the transect samples. The transects provided information on the relative abundances of the species on the island, while the sweep gave the total species number on the island. These data were collected in 2007 and 2008 and pooled to get a more complete accounting for the species number of each island. The lists of species found on each island is presented in Table 6.1.

| Big Woods (Mainland) | Big Island | Little Big Island |
|---|---|---|
| *Acer rubrum* | *Acer rubrum* | *Acer rubrum* |
| *Acer saccharum* | *Ailanthus altissmia* | *Amelanchier arborea* |
| *Ailanthus altissima* | *Amelanchier arborea* | *Carya cordiformis* |
| *Amelanchier arborea* | *Carya cordiformis* | *Carya glabra* |
| *Betula alleghaniensis* | *Carya glabra* | *Cornus florida* |
| *Carya cordiformis* | *Carya ovata* | *Elaeaguns umbellata* |
| *Carya glabra* | *Cornus floria* | *Hamamelis virginiana* |
| *Carya ovata* | *Elaeagnus umbellata* | *Populus grandidentata* |
| *Celtis occidentalis* | *Hamamelis virginiana* | *Prunus serotina* |
| *Cornus florida* | *Lonicera tatarica* | *Quercus alba* |
| *Elaeagnus umbellata* | *Malus sp* | *Quercus velutina* |
| *Fagus grandifolia* | *Ostrya virginiana* | *Sassafras albidum* |
| *Fraxinus americana* | *Populus grandidentata* | *Ulmus americana* |
| *Hamemelis virginiana* | *Prunus serotina* | |
| *Juglans nigra* | *Prunus virginiana* | |
| *Lonicera tatarica* | *Quercus alba* | |
| *Malus sp* | *Quercus velutina* | |
| *Ostrya virginiana* | *Rhus sp* | |
| *Populus grandidentata* | *Sassafras albidum* | |
| *Prunus serotina* | *Ulmus americana* | |
| *Prunus virginiana* | | |
| *Quercus alba* | | |
| *Quercus velutina* | | |
| *Rhus sp* | | |
| *Robinia pseudoacacia* | | |
| *Sassafras albidum* | | |
| *Thuja occidentalis* | | |
| *Tilia Americana* | | |

| *Ulmus americana* | | |
|---|---|---|
| Duloticus East Island | Duloticus West Island | Bee Island |
| *Acer rubrum* | *Acer rubrum* | *Acer rubrum* |
| *Amelanchier arborea* | *Amelanchier arborea* | *Amelanchier arborea* |
| *Carya glabra* | *Carya glabra* | *Carya glabra* |
| *Cornus floria* | *Carya ovata* | *Carya ovata* |
| *Elaeagnus umbellata* | *Cornus floria* | *Elaeagnus umbellata* |
| *Fraxinus americana* | *Elaeagnus umbellata* | *Hamamelis virginiana* |
| *Hamamelis virginiana* | *Hamamelis virginiana* | *Ostrya virginiana* |
| *Populus grandidentata* | *Ostrya virginiana* | *Populus grandidentata* |
| *Prunus serotina* | *Prunus serotina* | *Prunus serotina* |
| *Quercus alba* | *Quercus alba* | *Quercus alba* |
| *Quercus velutina* | *Quercus velutina* | *Quercus alba* |
| *Sassafras albidum* | *Ulmus americana* | *Ulmus americana* |
| *Tilia Americana* | | |
| *Ulmus americana* | | |
| Hourglass North Island | Hourglass South Island | Period Island |
| *Amelanchier arborea* | *Acer rubrum* | *Carya glabra* |
| *Carya glabra* | *Amelanchier arborea* | *Elaeagnus umbellata* |
| *Elaeagnus umbellata* | *Carya glabra* | *Prunus serotina* |
| *Hamamelis virginiana* | *Elaeagnus umbellata* | *Quercus velutina* |
| *Quercus alba* | *Hamamelis virginiana* | |
| *Quercus velutina* | *Prunus serotina* | |
| *Sassafras albidum* | *Quercus alba* | |
| *Tilia Americana* | *Quercus velutina* | |
| *Ulmus americana* | | |

Table 6.1: Species lists for the Big Swamp hummocks—our putative "islands."

To resample the transects we randomly selected 100 individuals from the transect(s) on a given island and then 100 individuals from a randomly place "transect" on the Big Woods mainland of the same size as the island transect(s). We repeated this process 1000 times to find the difference in number of species for each island samples compared to similar samples of the mainland. This difference was compared to the distance between the island and mainland and the area of each island. The distance to the mainland was taken as the distance from the northern edge of each island to the northern edge of the swamp. The area to the south of the swamp has only recently been reforested after a long history of grazing and agriculture, while the

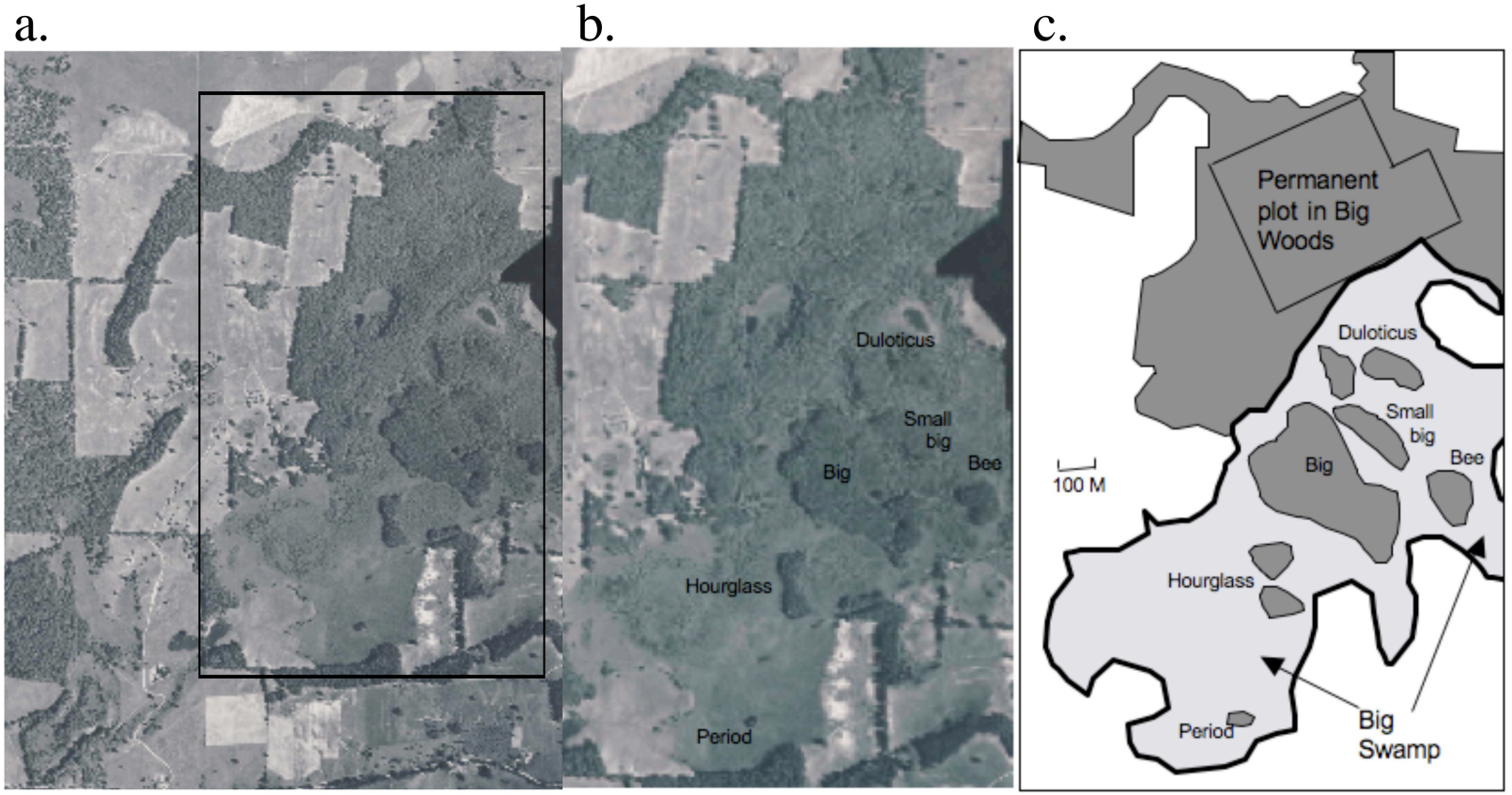


Figure 6.1: (a) An aerial photograph of the study region from 1940. The area to the north of the swamp is heavily forested, while that to the south is largely grazing land. (b) A close up from this photograph highlighting the islands in the swamp and the forested area to the north. (c) A cartoon representation of the photograph in (b).

| Name | Area ($m^2$) | Distance (m) | Number of Species |
|---|---|---|---|
| Big | 80571 | 66 | 20 |
| Little Big | 15003 | 199 | 14 |
| Bee | 12780 | 464 | 12 |
| Duloticus East | 10558 | 84 | 12 |
| Duloticus West | 7224 | 164 | 14 |
| Hourglass North | 6665 | 371 | 10 |
| Hourglass South | 5560 | 454 | 8 |
| Period | 1575 | 769 | 4 |

Table 6.2: The area, distance to the mainland, and number of species for each of the Big Swamp hummocks.

area to the north has been continuously forested at least since 1940 (see Figure 6.1) and considered to be the main source area. The areas were estimated when we conducted the transects in October 2008. The size of the islands is variable expanding in dry times, during the driest Duloticus east and west and Hourglass south and north each form single islands. The area and distance to the mainland for each island are reported in Table 6.2.

This resampling was then redone separately with two subgroups of species. The first, called the "old" species, included the five "canopy" species which have formed canopy of the Big Woods forest currently and before European colonization: *Q. alba*, *Q. velutina*, *C. glabra*, *C. ovata* and *C. cordiformis*. The second group, called the "young" species included all others, which maybe have been present in the Big Woods before European colonization but have most likely greatly increased their numbers (Abrams, 1998; Zhang et al., 2000; Heitzman et al., 2007; McDonald et al., 2003; Dickmann and Leefers, 2006). This will allow us to examine the temporal scale of island colonization.

## 6.3 Results

Our results confirm the prediction of the theory of island biogeography; larger island had more species and islands closer to the mainland had more species (Fig-

ure 6.2). In addition resamples of the transects of the four islands closest to the mainland—all less than 250m away—did not have a significantly different number of species than Big Woods samples of the same size (Figure 6.3). On the other hand, Big Woods resamples had significantly more species than resamples of the transects of the four islands farther than 250m away from the mainland (Figure 6.3). The Big Woods samples had between, on average, one to three-and-a-half more species than the island samples.

This difference is species number was solely driven by the difference in the number of "young" species. The Big Woods resamples had significantly more "young" species than the island resamples for the four farthest islands (Figure 6.4). While, for all islands, no matter their distance from the mainland, there was no statistical difference between the number of "old" species in the island resamples and in the Big Woods resamples (Figure 6.4).

## 6.4 Discussion

These results suggest that the hummocks located at a distance greater than about 250m function biologically as islands, while the closer islands, even though they are not contiguous, are functioning biologically as extensions of the forest. Thus nearby islands are recolonized at a rate not that much different than the mainland recolonizes local extensions within itself, while the furthest island recolonization rates are much lower resulting in the lower species numbers.

Since the long term history of the area is well-known, we are able to further tease out some of the island-like patterns. Specifically, since the *Quercus* overstory has been in existence for 150 years or more, and the distinct assemblage of understory has much more recently been dispersing into the overall area (we estimate, from cores, about 30–40 years in process), we can separate the large trees from the small ones and redo the above analysis. These results show that for the more recent species the

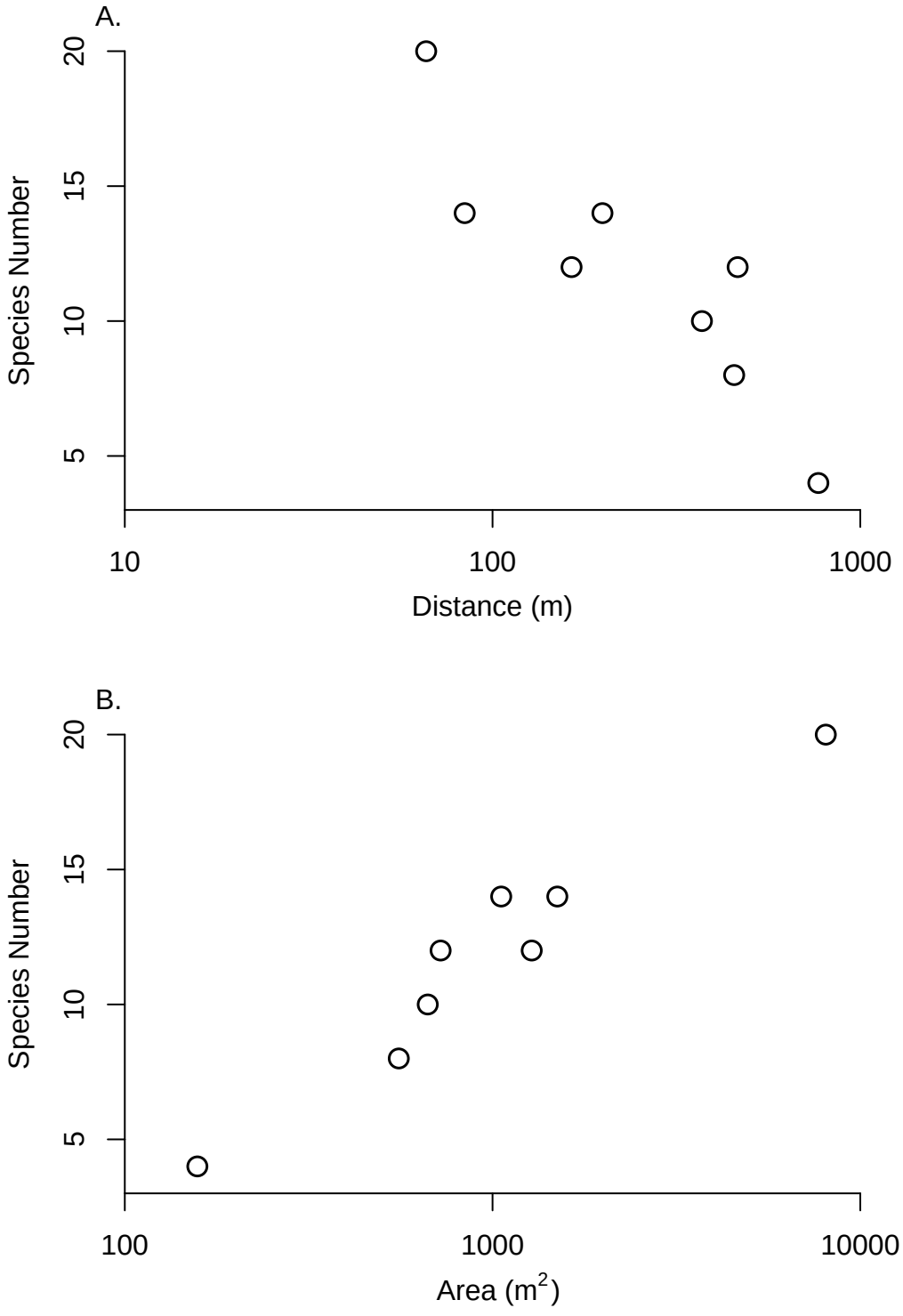


Figure 6.2: The total number of species on each island versus that island's (A) distance to the mainland and (B) area.

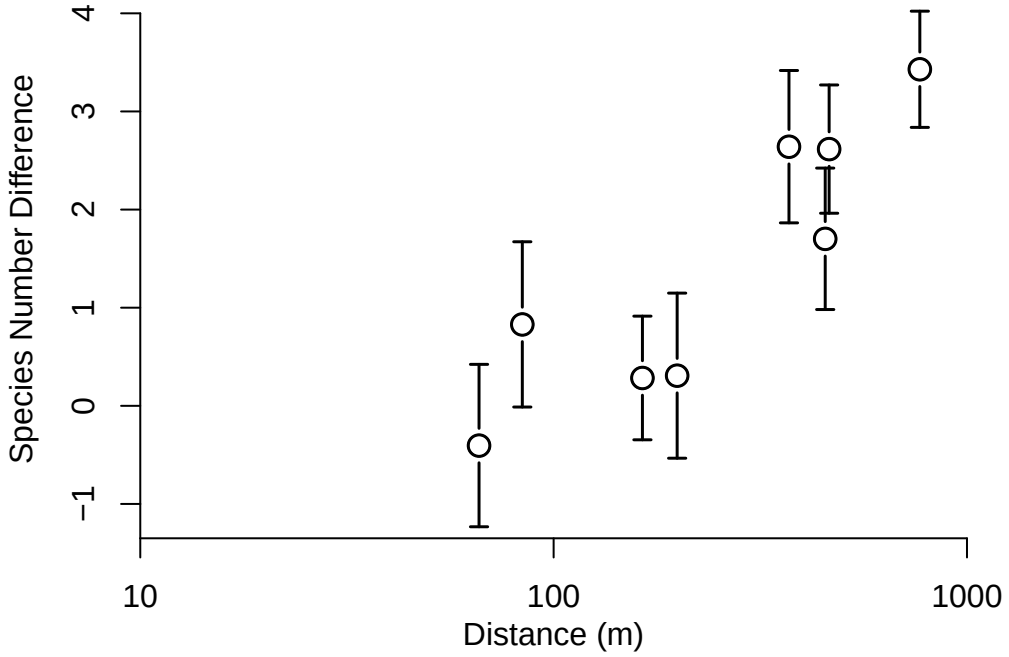


Figure 6.3: The relationship between island distance from mainland and the number of species in Big Woods samples minus the number in island transect resamples. Bars indicate the standard error.

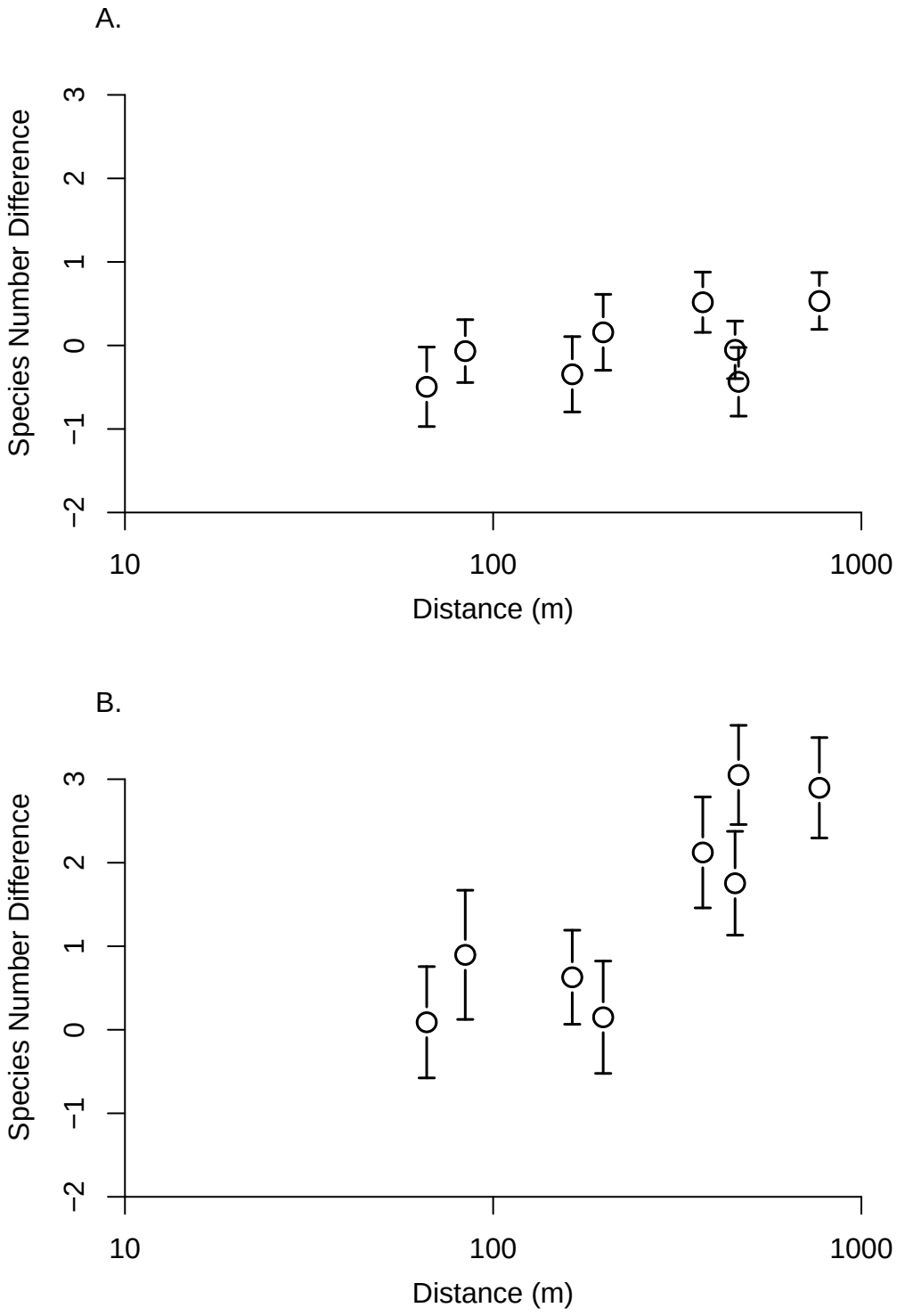


Figure 6.4: The relationship between island distance from the mainland and the number of species in the Big Woods samples minus the number in the island transects resamples broken up by species type. Bars indicate the standard error. (a) For "old" species and (b) for "young" species, see Methods for description of "old" and "young" species.

hummocks look even more like biological islands, but for the older species there is no relationship between distance and proportion. This may suggest that the island pattern may be a temporary phenomenon until the more recent species in the forest have time to colonize the farther islands.

This could also be explained by a stepping-stone model in which are farthest islands are colonized from other islands not the mainland. This process could take many decades to complete, in which case species which have a long history on the mainland have had time to 'step' out to the farthest island, while those whose numbers have increased only recently have not had time.

The procedure of looking for pattern as a signal of the island biogeographic process could be a useful way to assess the impact of habitat fragmentation in human-impacted systems. It could be used to determine if a system of fragmented habitat function as biological islands, and more specifically for which segment of the biota they do. It may be possible to use such a technique to assess matrix quality generally, or, if known, the effect of particular constructs of the matrix (row cropping versus pastures, for example).

# BIBLIOGRAPHY

# BIBLIOGRAPHY


Abrams, M. D. 1992. Fire and the development of oak forests. BioScience 42:346–353.

Abrams, M. D. 1998. The red maple paradox: what explains the widespread expansion of red maple in eastern forests? BioScience 48:355–364.

Anderson, G. J. and Hill, J. D. 2002. Many to flower, few to fruit: the reproductive biology of *Hamamelis virginana* (Hamamelidaceae). American Journal of Botany 89:67–78.

Augspurger, C. K. 1984. Seedling survival of tropical tree species: interactions of dispersal distance, light-gaps, and pathogens. Ecology 65:1705–1712.

Bascompte, J. and Solé, R. V. 1994. Spatially induced bifurcations in a single-species population dynamics. Journal of Animal Ecology 63:256–264.

Besuchet, C., Burckhardt, D. H., and Löbl, I. 1987. The "Winkler/Moczarski" eclector as an efficient extractor for fungus and litter coleoptera. The Coleopterists Bulletin 41:392–394.

Bond, W. J., Midgley, J., and Vlok, J. 1988. When is an island not an island? Insular effects and their causes in fynbos shrublands. Oecologia 77:515–521.

Brown, J. H. and Kodric-Brown, A. 1977. Turnover rates in insular biogeography: effect of immigration on extinction. Ecology 58:445–449.

Castets, V., Dulos, E., Boissonade, J., and De Kepper, P. 1990. Experimental evidence for a sustained standing Turing-type nonequilibrium chemical pattern. Physical Review Letters 64:2953–2956.

Clark, D. A. and Clark, D. B. 1984. Spacing dynamics of a tropical rain forest tree: evaluation of the Janzen–Connell model. American Naturalist 124:769–788.

Clark, W. E. 1987. Revision of the nearctic species of *Pseudanthonomus* Dietz (Coleoptera: Curculionidae). The Coleopterists Bulletin 41:263–285.

Clauset, A., Rohilla, C., and Newman, M. E. J. 2009. Power-law distributions and empirical data. SIAM Review 51:661–703.

Cleveland, W. S. and Devlin, S. J. 1988. Locally-weighted regression: an approach to regression by local fitting. Journal of the American Statistical Association 83:596–610.

Condit, R., Ashton, P. S., Baker, P., Bunyavejchewin, S., Gunatilleke, S., Gunatilleke, N., Hubbell, S. P., Foster, R. B., Itoh, A., LeFrankie, J. V., Lee, H. S., Losos, E., Manokaran, N., Sukumar, R., and Yamakura, T. 2000. Spatial patterns in the distribution of tropical tree species. Science 288:1414–1418.

Connell, J. H., 1971. On the role of natural enemies in preventing competitive exclusion in some marine animals and in rain forest trees. Pages 298–313 *in* Dynamics of Populations. Centre for Agricultural Publishing and Documentation, Wageningen.

Connell, J. H. 1978. Diversity of tropical rain forests and coral reefs. Science 199:1302–1310.

De Steven, D. 1981. Abundance and survival of a seed-infesting weevil, *Pseudanthonomus hamamelidis* (Coleoptera: Curculionidae), on its variable-fruiting host plant, witch-hazel (*Hamamelis virginiana*). Ecological Entomology 6:387–396.

De Steven, D. 1982. Seed production and seed mortality in a temperate forest shrub (witch-hazel, *Hamamelis virginana*). Journal of Ecology 70:437–443.

De Steven, D. 1983*a*. Floral ecology of witch-hazel (*Hamamelis virginana*). Michigan Botanist 22:163–171.

De Steven, D. 1983*b*. Reproductive consequences of insect seed predation in *Hamamelis virginana*. Ecology 64:89–98.

Dickmann, D. I. and Leefers, L. A., 2006. The Forests of Michigan. University of Michigan Press, Ann Arbor, MI.

Doebeli, M. and Killingback, T. 2003. Metapopulation dynamics with quasi-local competition. Theoretical Population Biology 64:397–416.

Durrett, R. and Levin, S. 1994. The importance of being discrete (and spatial). Theoretical Population Biology 46:363–394.

Earn, D. J. D., Levin, S. A., and Rohani, P. 2000. Coherence and conservation. Science 290:1360–1364.

Engelbrecht, B. M. J., Comita, L. S., Condit, R., Kursar, T. A., Tyree, M. T., Turner, B. L., and Hubbell, S. P. 2007. Drought sensitivity shapes species distribution patterns in tropical forests. Nature 447:80–82.

Enquist, B. J., West, G. B., and Brown, J. H. 2009. Extensions and evaluations of a general quantitative theory of forest structure and dynamics. Proceedings of the National Academy of Science 106:7046–7051.

Fisher, B. L. 1999. Improving inventory efficiency: a case study of leaf-litter ant diversity in Madagascar. Ecological Applications 9:714–731.

Hastings, A. 1992. Age dependent dispersal is not a simple process: density dependence, stability and chaos. Theoretical Population Biology 41:388–400.

Heitzman, E., Grell, A., Spetich, M., and Starkey, D. 2007. Changes in forest structure associated with oak decline in severely impacted areas of northern Arkansas. Southern Journal of Applied Forestry 31:17–22.

Hille Ris Lambers, J., Clark, J. S., and Beckage, B. 2002. Density-dependent mortality and the latitudinal gradient in species diversity. Nature 417:732–735.

Howe, H. F. 1989. Scatter- and clump-dispersal and seedling demography: hypothesis and implications. Oecologia 79:417–426.

Huffaker, C. B. 1958. Experimental studies on predation: dispersion factors and predator-prey oscillations. Hilgardia: A Journal of Agricultural Science 27:795–834.

Janzen, D. H. 1970. Herbivores and the number of tree species in tropical forests. American Naturalist 104:501–528.

Jedlicka, J. and Vandermeer, J. 2004. Gypsy moth defoliation of oak trees and a positive response of red maple and black cherry: an example of indirect interaction. American Midland Naturalist 152:231–236.

Kéfi, S., Rietkerk, M., Alados, C. L., Papanastasis, Y. P. V. P., ElAich, A., and de Ruiter, P. C. 2007. Spatial vegetation patterns and imminent desertification in Mediterranean arid ecosystems. Nature 449:213–217.

Klausmeier, C. A. 1999. Regular and irregular patterns in semiarid vegetation. Nature 284:1826–1828.

MacArthur, R. H. and Wilson, E. O., 1967. The Theory of Island Biogeography. Princeton University Press, Princeton.

May, R. M., 1974. Stability and complexity in model ecosystems. Princeton University Press, Princeton.

McDonald, R. I., Peet, R. K., and Urban, D. L. 2003. Spatial pattern of *Quercus* regeneration limitation and *Acer rubrum* invasion in a Piedmont forest. Journal of Vegetation Science 14:441–450.

Molofsky, J. and Bever, J. D. 2002. A novel theory to explain species diversity in landscapes: positive frequency dependence and habitat suitability. Proceedings of the Royal Society B: Biological Sciences 269:2389–2393.

Murray, J. D. 1981. A pre-pattern formation mechanism for animal coat markings. Journal of Theoretical Biology 88:161–199.

Packer, A. and Clay, K. 2000. Soil pathogens and spatial patterns of seedling mortality in a temperate tree. Nature 404:278–281.

Packer, A. and Clay, K. 2003. Soil pathogens and *Prunus serotina* seedlings and saplings growth near conspecific trees. Ecology 84:108–119.

Pascual, M. 1999. Diffusion-induced chaos in a spatial predator-prey system. Proceedings of the Royal Society London B: Biological Sciences 251:1–7.

Pascual, M., Roy, M., Guichard, F., and Flierl, G. 2002. Cluster size distributions: signatures of self-organization in spatial ecologies. Philosophical Transactions of the Royal Society of London Series B 357:657–666.

Perfecto, I. and Vandermeer, J. 2008. Spatial pattern and ecological process in the coffee agroforestry system. Ecology 89:915–920.

Reinhart, K. O., Packer, A., Van der Putten, W. H., and Clay, K. 2003. Plant-soil biota interactions and spatial distribution of black cherry in its native and invasive ranges. Ecology Letters 6:1046–1050.

Reinhart, K. O., Royo, A. A., Van Der Putten, W. H., and Clay, K. 2005. Soil feedback and pathogen activity in *Prunus serotina* throughout its native range. Journal of Ecology 93:890–898.

Rietkerk, M., Boerlijst, M. C., van Langevelde, F., HilleRisLambers, R., van de Koppel, J., Kumar, L., Prins, H. H. T., and de Roos, A. M. 2002. Self-organization of vegetation in arid ecosystems. American Naturalist 160:524–530.

Rietkerk, M., Dekker, S. C., de Ruiter, P. C., and van de Koppel, J. 2004*a*. Self-organized patchiness and catastrophic shifts in ecosystems. Science 305:1926–1929.

Rietkerk, M., Dekker, S. C., Wassen, M. J., Verkroost, A. W. M., and Bierkens, M. R. P. 2004*b*. A putative mechanism for bog patterning. American Naturalist 163:699–708.

Rohani, P., Godfray, H., and Hassell, M. P. 1994. Aggregation and the dynamics of host-parasitoid systems: a discrete-generation model with within-generation redistribution. American Naturalist 144:491–509.

Rohani, P., May, R. M., and Hassell, M. P. 1996. Metapopulations and equilibrium stability: the effects of spatial structure. Journal of Theoretical Biology 181:97–109.

Satnoianu, R. A., Menzinger, M., and Maini, P. K. 2000. Turing instabilities in general systems. Journal of Mathematical Biology 41:493–512.

Scheffer, M. and Carpenter, S. R. 2003. Catastrophic regime shifts in ecosystems: linking theory to observation. Trends in Ecology and Evolution 18:648–656.

Seidler, T. G. and Plotkin, J. B. 2006. Seed dispersal and spatial pattern in tropical trees. PLoS Biology 4:e344.

Simberloff, D. S. and Abele, L. G. 1976. Island biogeography theory and conservation practice. Science 191:285–286.

Solé, R. V. and Manrubia, S. C. 1995. Are rainforests self-organized in a critical state? Journal of Theoretical Biology 173:31–40.

Solé, R. V., Manrubia, S. C., Benton, M., Kauffman, S., and Bak, P. 1999. Criticality and scaling in evolutionary ecology. Trends in Ecology and Evolution 14:156–160.

Turing, A. M. 1952. The chemical basis of morphogenesis. Philosophical Transactions of the Royal Society of London Series B 237:37–72.

van de Koppel, J., Rietkerk, M., Dankers, N., and Herman, P. M. J. 2005. Scale-dependent feedback and regular spatial patterns in young mussel beds. American Naturalist 165:E66–E77.

Vandermeer, J. H. and Kaufmann, A. 1998. Models of coupled populations oscillators using 1-d maps. Journal of Mathematical Biology 37:178–202.

Voss, E. G., 1985. Michigan Flora, Volume 2: Dicots. Cranbrook Institute of Science, Bloomfield Hills, MI.

West, G. B., Enquist, B. J., and Brown, J. H. 2009. A general quantitative theory of forest structure and dynamics. Proceedings of the National Academy of Science 106:7040–7045.

White, E. P., Enquist, B. J., and Green, J. L. 2008. On estimating the exponent of power-law frequency distributions. Ecology 89:905–912.

Wills, C., Harms, K. E., Condit, R., King, D., Thompson, J., He, F., Muller-Landau, H. C., Ashton, P., Losos, E., Comita, L., Hubbell, S., LaFrankie, J., Bunyavejchewin, S., Dattaraja, H. S., Davies, S., Esufali, S., Foster, R., Gunatilleke, N., Gunatilleke, S., Hall, P., Itoh, A., John, R., Kiratiprayoon, S., Loo de Lao, S., Massa, M., Nath, C., Noor, M. N. S., Kassim, A. R., Sukumar, R., Suresh, H. S., Sun, I.-F., Tan, S., Yamakure, T., and Zimmerman, J. 2006. Nonrandom processes maintain diversity in tropical forests. Science 311:527–531.

Zhang, Q., Pregitzer, K. S., and Reed, D. D. 2000. Historical changes in the forests of the Luce District of the Upper Peninsula of Michigan. American Midland Naturalist 143:94–110.